

Continuum Limits of Ollivier’s Ricci Curvature on data clouds: pointwise consistency and global lower bounds

Nicolás García Trillos¹ and Melanie Weber²

¹Department of Statistics, University of Wisconsin-Madison

²Harvard University

July 6, 2023

Abstract

Let $\mathcal{M} \subseteq \mathbb{R}^d$ denote a low-dimensional manifold and let $\mathcal{X} = \{x_1, \dots, x_n\}$ be a collection of points uniformly sampled from \mathcal{M} . We study the relationship between the curvature of a random geometric graph built from \mathcal{X} and the curvature of the manifold \mathcal{M} via continuum limits of Ollivier’s discrete Ricci curvature. We prove pointwise, non-asymptotic consistency results and also show that if \mathcal{M} has Ricci curvature bounded from below by a positive constant, then the random geometric graph will inherit this global structural property with high probability. We discuss applications of the global discrete curvature bounds to contraction properties of heat kernels on graphs, as well as implications for manifold learning from data clouds. In particular, we show that the consistency results allow for characterizing the intrinsic curvature of a manifold from extrinsic curvature estimators.

1 Introduction

The problem of identifying geometric structure in data is central to Machine Learning and Data Science. A frequently encountered structure is *low-dimensionality*, where high-dimensional data is assumed to lie on or near a low-dimensional manifold (*manifold hypothesis*). Let $\mathcal{X} \subset \mathbb{R}^d$ denote such a data set of size n and $\mathcal{M} \subseteq \mathbb{R}^d$ a low-dimensional manifold from which \mathcal{X} was sampled. Given \mathcal{X} , but without prior knowledge of \mathcal{M} , what can we say about the *intrinsic* geometry of \mathcal{M} ? In particular, what can we learn about intrinsic notions of curvature of \mathcal{M} from \mathcal{X} ? One of the central goals of this paper is to study this question through the lens of discrete Ricci curvature. Traditionally, curvature has been studied in continuous spaces such as Riemannian manifolds. Several different notions of curvature relate to the local and global geometric properties

of manifolds. *Ricci curvature*, is a classical concept in Riemannian geometry which in particular determines the volume growth of geodesic balls and that is closely connected to functional inequalities. In this paper, we study a *discrete* notion of Ricci curvature originally defined by Ollivier [36] and its relationship to the classical Ricci curvature on \mathcal{M} . More specifically, we study the relationship between the curvature of a *random geometric graph* (short: *RGG*) built from \mathcal{X} and the curvature of the manifold \mathcal{M} . A RGG G is constructed from a sample \mathcal{X} by connecting points with a *distance* of at most ε with an edge; as we will discuss below, the choice of distance function plays an important role in our results.

In more concrete terms, we are interested in the following two questions:

Problem 1. *Can we give non-asymptotic error bounds for the pointwise estimation of the curvature of \mathcal{M} from that of G ?*

Problem 2. *If the manifold \mathcal{M} has Ricci curvature bounded from below by a given constant, will a RGG inherit this global structural property with high probability? What are some consequences of the resulting discrete curvature lower bounds?*

We will discuss both questions in two different settings. In the first, which is of mostly theoretical value, we have access to the pairwise geodesic distances of points in \mathcal{X} , i.e., in G two points are connected by an edge if they are within distance ε from each other along the manifold. In the second setting, we have no access to geodesic distances but we assume to instead have access to sufficiently accurate data-driven approximations thereof. In studying these two problems we will be able to provide theoretical insights into the relationship between discrete and continuous Ricci curvature and deliver consistent continuum limits of Ollivier’s Ricci curvature on data clouds. Recall that a positive global lower bound on the Ricci curvature has several important implications for the manifold’s geometry, including a bound on the diameter of complete manifolds (Bonnet-Myers [33]), as well as consequences for the coupling of random walks, which we will discuss below. We will explore some novel implications of having discrete curvature lower bounds on the behavior of graph Laplacians built over G . For example, the results presented in section 7.1 are novel in the literature of graph Laplacians and do not follow from existing discrete-to-continuum consistency results.

1.1 Outline

In order to precisely state our main results, we first present some background material. In particular, in section 2.1 we present some background on differential geometry and, importantly, introduce the notions of Ricci curvature, parallel transport, and second fundamental form of an embedded manifold; all these notions will be used in the sequel. Then, in section 2.2, we discuss the notion of Ollivier Ricci curvature for triplets $(\mathcal{U}, d, \mathbf{m})$ consisting of a metric space (\mathcal{U}, d) and a Markov kernel \mathbf{m} over \mathcal{U} ; we will discuss a special setting where \mathcal{U}

is a Riemannian manifold \mathcal{M} and discuss the connection between the induced Ollivier Ricci curvature and the classical Ricci curvature discussed in section 2.1. In section 2.3 we introduce the RGGs G over \mathcal{X} that we will study throughout the paper and define associated discrete Ollivier Ricci curvatures up to the choice of a metric d_G over \mathcal{X} . The metric d_G will be explicitly defined in section 3.3, right after discussing the approximation of geodesic distances over \mathcal{M} from data at the beginning of section 3.

In section 4 we present our main theoretical results: in section 4.1 our point-wise consistency results (Theorems 8 and 9), and in section 4.2 our global lower bounds (Theorems 10 and 13). In section 4.3 we illustrate the recovery of Ricci curvature from data with a simple numerical experiment.

In section 5 we discuss some related literature.

In section 6 we present the proofs of our main results.

In section 7 we present a brief discussion of some applications of our main theoretical results. One such application is discussed in section 7.1, where we study the Lipschitz contractivity of graph heat kernels over data clouds sampled from manifolds with positive curvature. In section 7.2 we discuss some of the avenues that our main results may open up in the field of manifold learning.

We wrap up the paper in section 8 with some conclusions and some discussion on avenues for future research directions.

2 Background and Notation

2.1 Notions from Differential Geometry

We start by recalling some basic definitions and tools from differential geometry that we have collected from Chapters 0-4 and 6 in [14]. This will also give us the opportunity to introduce some notation that we use in the sequel.

An m -dimensional *manifold* \mathcal{M} is a locally Euclidean space of dimension m with a differentiable structure. We use $T_x\mathcal{M}$ to denote the tangent plane at the point $x \in \mathcal{M}$. Throughout the paper we will only consider smooth, connected, compact *Riemannian* manifolds without boundary. These are manifolds endowed with a smoothly varying inner product structure $g = \{g_x\}_{x \in \mathcal{M}}$ defined over their tangent planes. The geodesic distance $d_{\mathcal{M}}$ between two points $x, y \in \mathcal{M}$ is defined according to

$$d_{\mathcal{M}}(x, y) = \inf_{\gamma: [0,1] \rightarrow \mathcal{M}} \int_0^1 \sqrt{g_{\gamma(t)}(\dot{\gamma}(t), \dot{\gamma}(t))} dt,$$

where the inf ranges over all smooth paths connecting x to y . Important notions in Riemannian geometry such as geodesic curves (in particular length minimizers) and curvature are defined in terms of *connections* or *covariant derivatives*. Informally, given a smooth curve γ on \mathcal{M} , the covariant derivative $\nabla_{\dot{\gamma}}$ is an operator, satisfying some linearity and Leibnitz product rule properties, mapping vector fields along γ into vector fields along γ . Among the multiple choices of

connection that can be defined over a manifold, we will work with the Levi-Civita connection, which satisfies some additional compatibility conditions with the Riemannian structure of the manifold; see details in Chapter 2 in [14].

In general, a geodesic is a smooth path $\gamma : [0, 1] \rightarrow \mathcal{M}$ satisfying $\nabla_{\dot{\gamma}}\dot{\gamma} = 0$. It is possible to show that for every $x \in \mathcal{M}$ and every $v \in T_x\mathcal{M}$ there exists a unique geodesic γ satisfying $\gamma(0) = x$ and $\dot{\gamma}(0) = v$. We may use this fact to define the *exponential map* $\exp_x : T_x\mathcal{M} \rightarrow \mathcal{M}$, which maps v to $\gamma(1)$ for γ the geodesic starting at x in the direction v . It can be shown that there exists a real number $\iota_{\mathcal{M}} > 0$, known as \mathcal{M} 's *injectivity radius*, for which $\exp_x : B(0, \varepsilon) \subseteq T_x\mathcal{M} \rightarrow B_{\mathcal{M}}(x, \varepsilon)$ is a diffeomorphism for all $x \in \mathcal{M}$ and all $\varepsilon < \iota_{\mathcal{M}}$; here and in the remainder, we use $B_{\mathcal{M}}(x, \varepsilon)$ to denote the ball of radius ε around x when \mathcal{M} is endowed with $d_{\mathcal{M}}$ and $B(0, \varepsilon)$ is the m -dimensional Euclidean ball of radius ε . The inverse of \exp_x , the *logarithmic map*, will be denoted by $\log_x : B_{\mathcal{M}}(x, \varepsilon) \subseteq \mathcal{M} \rightarrow B(0, \varepsilon) \subseteq T_x\mathcal{M}$. For any two points x, y with $d_{\mathcal{M}}(x, y) < \iota_{\mathcal{M}}$, the unique minimizing geodesic between x and y (i.e., a minimizer in the definition of $d_{\mathcal{M}}(x, y)$) is given by $\gamma : t \in [0, 1] \mapsto \exp_x(tv)$ where $v = \frac{\log_x(y)}{|\log_x(y)|}$. This minimizing geodesic can be reparametrized so that it is unit speed (i.e., $\dot{\gamma}(0)$ has norm one) in which case γ maps the interval $[0, d_{\mathcal{M}}(x, y)]$ into \mathcal{M} . From now on we will refer to this curve as the unit speed geodesic between x and y .

With the notion of Levi-Civita connection we can also introduce the concept of *parallel transport*, one important notion that allows us to relate tangent vectors at different points on \mathcal{M} . Precisely, let $\gamma : [0, a] \rightarrow \mathcal{M}$ be a smooth curve on \mathcal{M} and let $x = \gamma(0)$ and $y = \gamma(a)$. Given $v \in T_x\mathcal{M}$, we define $V(t) \in T_{\gamma(t)}\mathcal{M}$, the parallel transport of v along γ , to be the (unique) solution to the equation $\nabla_{\dot{\gamma}(t)}V = 0$ with initial condition $V(0) = v$. We will be particularly interested in the case where γ is the unit speed geodesic between x and y (sufficiently close to each other) and we will denote by P_{xy} the map $P_{xy} : T_x\mathcal{M} \rightarrow T_y\mathcal{M}$ defined as $v \in T_x\mathcal{M} \mapsto V(d_{\mathcal{M}}(x, y)) \in T_y\mathcal{M}$.

We can locally characterize the curvature of the manifold \mathcal{M} in a neighborhood of a point $x \in \mathcal{M}$ via *Ricci curvature*. Formally, let $v \in T_x\mathcal{M}$ denote a unit vector and $\{u_1, \dots, u_{m-1}, v\}$ an orthonormal basis for $T_x\mathcal{M}$. We define the *Ricci curvature* at x along the direction v as

$$\text{Ric}_x(v) := \frac{1}{m-1} \sum_{i=1}^{m-1} g(R(v, u_i)v, u_i), \quad (1)$$

where $R(u, v)w := \nabla_u\nabla_v w - \nabla_v\nabla_u w - \nabla_{[u, v]}w$, for $[u, v]$ the Lie Bracket between u and v . Furthermore, we can globally characterize \mathcal{M} 's geometry via *sectional curvature*, which is given by

$$K(u, v) := K_x(u, v) = \frac{g(R(u, v)u, v)}{|u|^2|v|^2 - (g(u, v))^2} \quad (2)$$

for $u, v \in T_x\mathcal{M}$ and $x \in \mathcal{M}$; here we use the notation $|u|^2 = g(u, u)$.

Let $x, y \in \mathcal{M}$ and let $\varepsilon > 0$ be smaller than the injectivity radius $\iota_{\mathcal{M}}$. We define $\mathcal{P} : B_{\mathcal{M}}(x, \varepsilon) \rightarrow B_{\mathcal{M}}(y, \varepsilon)$ the map given by

$$\mathcal{P}(\tilde{x}) = \exp_y(P_{xy}(\log_x(\tilde{x}))). \quad (3)$$

That is, \tilde{x} is mapped to x 's tangent plane and then transported to y 's tangent plane along the geodesic connecting x and y (unique if we assume $d_{\mathcal{M}}(x, y) < \iota_{\mathcal{M}}$) to finally be mapped to $B_{\mathcal{M}}(y, \varepsilon)$ via the exponential map at y . One important property of the diffeomorphism \mathcal{P} that we use in the sequel, originally due to Levi-Civita, is that if we form the quadrilateral illustrated in Figure 1, then the distance between \tilde{x} and \tilde{y} can be precisely characterized, up to correction terms of order 4, by the distance between x and y and \mathcal{M} 's sectional curvature at x . More precisely, we have the following result.

Proposition 1 (cf Proposition 6 in [36]). *Let $\varepsilon > 0$ be a number smaller than $\iota_{\mathcal{M}}$, the injectivity radius of \mathcal{M} . Let $x, y \in \mathcal{M}$ be such that $d_{\mathcal{M}}(x, y) < \iota_{\mathcal{M}}$ and let $\tilde{x} \in B_{\mathcal{M}}(x, \varepsilon)$ and $\tilde{y} := \mathcal{P}(\tilde{x})$ with \mathcal{P} as in (3). Then*

$$d_{\mathcal{M}}(\tilde{x}, \tilde{y}) = d_{\mathcal{M}}(x, y) \left(1 - \frac{(d_{\mathcal{M}}(x, \tilde{x}))^2}{2} (K(v, w) + O(\varepsilon + d_{\mathcal{M}}(x, y))) \right),$$

where $v = \frac{\log_x(y)}{|\log_x(y)|}$ and $w = \log_x(\tilde{x})$.

In the remainder we will consider *embedded submanifolds* \mathcal{M} of \mathbb{R}^d , which are defined as follows.

Definition 1 (Embedded submanifold (see, e.g., [4])). *We say that $\mathcal{M} \subseteq \mathbb{R}^d$ is a smooth embedded submanifold of \mathbb{R}^d of dimension m strictly less than d if for every $x \in \mathcal{M}$ there is a ball $B(x, r) \subseteq \mathbb{R}^d$ and a smooth function $h_x : B(x, r) \rightarrow \mathbb{R}^d$ (termed defining function), such that (i) $h_x(y) = 0$ iff $y \in \mathcal{M} \cap B(x, r)$ and (ii) $\text{rank } \nabla h_x(x) = d - m$.*

Moreover, the inner product g_x defined over $T_x\mathcal{M}$, the latter now seen as a subspace of \mathbb{R}^d , is the restriction of $\langle \cdot, \cdot \rangle$, the \mathbb{R}^d inner product, to $T_x\mathcal{M}$.

In the sequel we use the *second fundamental form* $\mathbb{I}_x(\cdot, \cdot)$ of the embedded manifold \mathcal{M} in order to discuss data driven approximations to the geodesic distance on \mathcal{M} . Let $N_x\mathcal{M}$ denote the normal space of \mathcal{M} , i.e., the orthogonal complement of $T_x\mathcal{M}$ in \mathbb{R}^d . The second fundamental form is given by the map $\mathbb{I}_x : T_x\mathcal{M} \times T_x\mathcal{M} \rightarrow N_x\mathcal{M}$ defined by $(u, v) \mapsto (\text{Id} - \text{Proj}_x)(\frac{d}{dt}V(t)|_{t=0})$. Here, $\text{Proj}_x : \mathbb{R}^d \rightarrow T_x\mathcal{M}$ denotes the orthogonal projection onto the tangent space; γ is a curve on \mathcal{M} with $\gamma(0) = 0$ and $\dot{\gamma}(0) = u$; V is a vector field along γ with $V(t) \in T_{\gamma(t)}\mathcal{M}$ satisfying $V(0) = v$.

Lastly, we define the *reach* of a manifold \mathcal{M} . Let $S \subset \mathbb{R}^d$ denote a closed subset and $\pi_S : \mathbb{R}^d \rightarrow S$ a map that sends $z \in \mathbb{R}^d$ onto its nearest neighbor in S . The reach $\tau_{\mathcal{M}}$ of \mathcal{M} is defined as the maximal neighborhood radius for which the projection $\pi_{\mathcal{M}}$ is well-defined, i.e., any point that has distance at most $\tau_{\mathcal{M}}$ from \mathcal{M} has a unique nearest neighbor on \mathcal{M} .

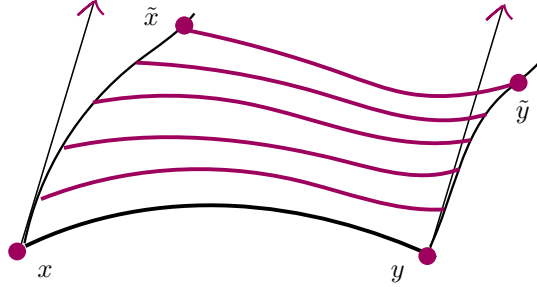


Figure 1: Levi-Civita parallelogram. The red lines represent geodesics.

Second fundamental form and reach are notions that are closely connected to the *extrinsic* curvature of a manifold. In contrast, Ricci curvature and sectional curvature are *intrinsic*. A standard way to visualize the difference between the two types of curvature is to imagine a circle drawn on a flat piece of paper, which one can think of as a one dimensional manifold \mathcal{M} embedded in \mathbb{R}^3 , and then the same circle after the paper has been rolled to form a cylinder, which can be thought of as a one dimensional manifold \mathcal{M}' embedded in \mathbb{R}^3 . While \mathcal{M} and \mathcal{M}' have the same intrinsic curvature (because the paper is not stretched when rolling it), their extrinsic curvature will be different.

2.2 Ollivier's Ricci curvature

Let (\mathcal{U}, d) be a metric space and let μ_1, μ_2 be two probability distributions over \mathcal{U} . Recall that the *1-Wasserstein distance* between μ_1, μ_2 is defined as

$$W_1(\mu_1, \mu_2) = \inf_{\pi \in \Gamma(\mu_1, \mu_2)} \int_{(x,y) \in \mathcal{U} \times \mathcal{U}} d(x,y) d\pi(x,y), \quad (4)$$

where $\Gamma(\mu_1, \mu_2)$ is the set of measures on $\mathcal{U} \times \mathcal{U}$ with marginals μ_1, μ_2 . Now, let \mathbf{m} denote a Markov kernel over \mathcal{X} , i.e., \mathbf{m} is a collection $\{m_x\}_{x \in \mathcal{U}}$ of probability measures over \mathcal{U} . The Ollivier Ricci curvature associated to the triplet $(\mathcal{U}, d, \mathbf{m})$ in direction (x, y) is given by [36]:

$$\kappa(x, y) := 1 - \frac{W_1(m_x, m_y)}{d(x, y)}. \quad (5)$$

Notice that, in general, the notion of Ollivier Ricci curvature only requires the structure of a metric space endowed with a (discrete-time) random walk. In the remainder of this section we will consider the case where \mathcal{U} is assumed to be a Riemannian manifold and discuss the relation between (5) and the geometric notion of Ricci curvature introduced in section 2.1. To do this we first need some definitions.

Definition 2 (Ollivier's Ricci curvature on manifolds [36]). *Let $d_{\mathcal{M}}(x, y)$ denote the geodesic distance in \mathcal{M} between x and y and let $B_{\mathcal{M}}(x, \varepsilon), B_{\mathcal{M}}(y, \varepsilon)$ be the*

closed balls of radius ε (a fixed parameter) around x and y , respectively (termed Ollivier balls). Let further

$$\mu_x^{\mathcal{M}}(z) = \frac{\text{vol}(z)|_{B_{\mathcal{M}}(x,\varepsilon)}}{\text{vol}(B_{\mathcal{M}}(x,\varepsilon))} \quad (6)$$

$$\mu_y^{\mathcal{M}}(z) = \frac{\text{vol}(z)|_{B_{\mathcal{M}}(y,\varepsilon)}}{\text{vol}(B_{\mathcal{M}}(y,\varepsilon))} \quad (7)$$

denote uniform measures on those neighborhoods. Then we define Ollivier's Ricci curvature between x and y as

$$\kappa_{\mathcal{M}}(x, y) = 1 - \frac{W_1(\mu_x^{\mathcal{M}}, \mu_y^{\mathcal{M}})}{d_{\mathcal{M}}(x, y)}. \quad (8)$$

Ollivier showed the following fundamental relationship between Ric and $\kappa_{\mathcal{M}}$:

Theorem 1 (Ollivier [36]).

$$\left| \kappa_{\mathcal{M}}(x, y) - \frac{\varepsilon^2}{2(m+2)} \text{Ric}_x(v) \right| \leq (C\varepsilon^2 d_{\mathcal{M}}(x, y) + C'\varepsilon^3), \quad (9)$$

where y is a point on the geodesic from x in direction v (of norm one) and ε is the radius of the Ollivier balls. C, C' are constants independent of m .

This theorem makes precise the intuition that random walks in \mathcal{M} starting at nearby points and suitably coupled draw closer together if the Ricci curvature is positive and further apart if the Ricci curvature is negative. It also provides the motivation for the definition of Ricci curvature of arbitrary triplets $(\mathcal{U}, d, \mathbf{m})$.

In section 6.1.3, we present the main steps in the proof of Theorem 1. This will give us the opportunity to introduce some key estimates and constructions that we use later in section 6 when proving our main results.

2.3 Curvature on Random Geometric Graphs

We recall the notion of a *random geometric graph* (short: RGG) on \mathcal{M} . Let vol denote \mathcal{M} 's volume form and let μ be the uniform probability measure over \mathcal{M} defined by

$$\mu(A) := \frac{\int_A d\text{vol}(x)}{\int_{\mathcal{M}} d\text{vol}(x)}$$

for all measurable subsets A of \mathcal{M} . Let $\mathcal{X} = \{x_i\}_{i=1}^n$ be a collection of i.i.d. samples from μ . In the sequel, we use μ_n to denote the empirical measure associated to these data points. Namely,

$$\mu_n := \frac{1}{n} \sum_{i=1}^n \delta_{x_i}.$$

We construct a random geometric graph $G_\varepsilon = (\mathcal{X}, w_\varepsilon)$ by connecting any pair of samples $x, y \in \mathcal{X}$ with an edge whenever their geodesic distance, or an approximation thereof, is less than ε . More precisely, we'll set w_ε to be either

$$w_\varepsilon(x, y) = w_{\varepsilon, \mathcal{M}}(x, y) := \begin{cases} 1 & \text{if } d_{\mathcal{M}}(x, y) \leq \varepsilon \\ 0 & \text{else,} \end{cases} \quad (10)$$

or

$$w_\varepsilon(x, y) = w_{\varepsilon, \mathcal{X}}(x, y) := \begin{cases} 1 & \text{if } \hat{d}_g(x, y) \leq \varepsilon \\ 0 & \text{else.} \end{cases} \quad (11)$$

The first setting, which uses the geodesic distance on \mathcal{M} , is only reasonable in applied settings where the manifold \mathcal{M} is known. In contrast, the second setting only presupposes having access to a function \hat{d}_g that serves as a data-driven local approximation for the geodesic distance $d_{\mathcal{M}}$. In section 3 we discuss some required properties for this approximation and highlight the need to work with approximations of $d_{\mathcal{M}}$ of high enough order if one desires to recover precise curvature information of the underlying manifold \mathcal{M} from the graph G_ε as $n \rightarrow \infty$.

Analogous to the continuous case, we can define Ollivier's Ricci curvature on the RGGs introduced above. In order to do so, we recall that we need two ingredients: a random walk over \mathcal{X} and a notion of distance over \mathcal{X} .

First, we introduce the graph Ollivier balls

$$B_G(x, \varepsilon) := \{z \in \mathcal{X} : w_\varepsilon(x, z) = 1\} \quad \forall x \in \mathcal{X}, \quad (12)$$

and we consider the family $\{\mu_x^G\}_{x \in \mathcal{X}}$ of uniform distributions

$$\mu_x^G(z) = \frac{1}{|B_G(x, \varepsilon)|}, \quad z \in B_G(x, \varepsilon). \quad (13)$$

Observe that the measures μ_x^G define the transition probabilities for a random walk on the RGG. The generator of the discrete-time Markov chain with transition probabilities given by $\{\mu_x^G\}_{x \in \mathcal{X}}$ is known in the literature as the *random walk graph Laplacian*; see [47].

Remark 2. Notice that the construction of the ball $B_G(x, \varepsilon)$ and its associated probability measure over \mathcal{X} , μ_x^G , continues to make sense for any arbitrary base point $x \in \mathcal{M}$, regardless of whether x is a data point in \mathcal{X} or not. This observation will be used in our theoretical analysis in subsequent sections.

The second ingredient needed to define Ollivier's Ricci curvature over G_ε is a distance function d_G over \mathcal{X} . Two specific choices for d_G , one useful when $d_{\mathcal{M}}$ is unknown and the other useful when $d_{\mathcal{M}}$ is known, will be discussed in section 3.3; both choices will endow \mathcal{X} with a suitable geodesic metric space structure. Either way, once d_G has been fixed, we can define, relative to the

family of measures $\{\mu_x^G\}_{x \in \mathcal{X}}$ (which in turn we recall depends on the choice of w_ε), the Ollivier Ricci curvature between points $x, y \in \mathcal{X}$ as

$$\kappa_G(x, y) := 1 - \frac{W_{1,G}(\mu_x^G, \mu_y^G)}{d_G(x, y)}. \quad (14)$$

In the above, $W_{1,G}(\mu_x^G, \mu_y^G)$ is the 1-Wasserstein distance induced by the metric d_G over \mathcal{X} . Precisely,

$$W_{1,G}(\mu_x^G, \mu_y^G) = \min_{\pi \in \Gamma(\mu_x^G, \mu_y^G)} \int d_G(\tilde{x}, \tilde{y}) d\pi(\tilde{x}, \tilde{y}). \quad (15)$$

3 Approximation of geodesic distances from data

One of the settings that we study in this paper assumes no access to pairwise geodesic distances $d_{\mathcal{M}}(x, y)$ ($x, y \in \mathcal{X}$) in our data set, but distances between points may still be computed in the ambient Euclidean space. In order to recover the manifold's intrinsic curvature information from the data in this setting, we will assume to have access to an oracle, data-driven estimator of $d_{\mathcal{M}}$, denoted \hat{d}_g , satisfying the following conditions.

Assumption 1. *The function $\hat{d}_g : \mathcal{M} \times \mathcal{M} \rightarrow [0, \infty)$ is assumed to be a symmetric function satisfying, with probability at least $1 - C \exp(-\zeta(\beta, n, \varepsilon))$, the following conditions:*

1. *For every $x, y \in \mathcal{M}$ satisfying $c\varepsilon \leq d_{\mathcal{M}}(x, y) \leq C\varepsilon$ or $c\varepsilon \leq \hat{d}_g(x, y) \leq C\varepsilon$, we have*

$$|d_{\mathcal{M}}(x, y) - \hat{d}_g(x, y)| \leq C_1 \beta \varepsilon^3 + C_2 \varepsilon^4. \quad (16)$$

2. *We have*

$$\hat{d}_g(x, y) \leq c\varepsilon \implies d_{\mathcal{M}}(x, y) \leq \frac{4}{3} c\varepsilon. \quad (17)$$

Here, $\zeta(n, \beta, \varepsilon)$ is assumed to be of the form $Cn^{q_1} \varepsilon^{q_2} \beta^{q_3}$ for positive powers $q_1, q_2, q_3 > 0$. In particular, $\zeta(n, \beta, \varepsilon) \rightarrow \infty$ as $n \rightarrow \infty$, whenever $\beta > 0$ and $\varepsilon > 0$ are fixed.

We have assumed the function $\hat{d}_g(x, y)$ to be symmetric, but it is not required to satisfy the other axioms of distance functions. Recall that \hat{d}_g has been used in the definition of the weights $w_{\varepsilon, \mathcal{X}}$ appearing in (11), and we will use it again in section 3.3 to define a data driven distance $d_{G, \mathcal{X}}$ over \mathcal{X} . The first condition in Assumption 1 states that, with high probability, \hat{d}_g approximates $d_{\mathcal{M}}$ locally with an error of order four, at least as long as the distance between points is not too small. In general, one should not expect the same type of error estimate for $d_{\mathcal{M}}$ at very small length scales, which is why we instead require condition 2, a much more reasonable assumption.

Remark 3. *The Euclidean distance is not a valid choice for \hat{d}_g since its error of approximation is only $O(\varepsilon^3)$; see the discussion in section 3.1.*

In sections 3.1 and 3.2 we discuss how the problem of constructing an admissible \hat{d}_g can be reduced to the problem of approximating the second fundamental form of \mathcal{M} from data and review some of the existing literature on this topic. In section 3.3, on the other hand, we introduce two geodesic distance functions d_G over \mathcal{X} that we may use to induce a Ricci curvature κ_G over the data cloud \mathcal{X} .

3.1 Estimation when geodesic distance for nearby points is not available

Although in the literature there already exist potential avenues for estimating $d_{\mathcal{M}}$ from data (see section 5), in this section we suggest an alternative approach that illustrates how it is possible to transform estimators for extrinsic geometric quantities into estimators for intrinsic ones. Our discussion will also allow us to illustrate why the Euclidean distance may not be a good enough estimator for $d_{\mathcal{M}}$ if one wishes to recover \mathcal{M} 's Ricci curvature from data.

Let $\gamma : [0, \infty) \rightarrow \mathcal{M} \subseteq \mathbb{R}^d$ be a unit speed geodesic in \mathcal{M} . We will assume without the loss of generality that $x = \gamma(0) = 0$. At least for small enough time $t \leq t_0$, we have:

$$d_{\mathcal{M}}(x, \gamma(t)) = t.$$

We now compare the above with

$$|x - \gamma(t)| = |\gamma(t)|,$$

the Euclidean distance between x and $\gamma(t)$. For that purpose we define the function

$$h(t) := t^2 - |\gamma(t)|^2, \quad t \in [0, t_0].$$

A direct computation using the fact that $\langle \dot{\gamma}(t), \dot{\gamma}(t) \rangle = 1$ reveals the following expressions for the first four derivatives of h :

$$h'(t) = 2t - 2\langle \dot{\gamma}(t), \gamma(t) \rangle,$$

$$h''(t) = -2\langle \ddot{\gamma}(t), \gamma(t) \rangle,$$

$$h'''(t) = -2\langle \ddot{\gamma}(t), \gamma(t) \rangle - 2\langle \ddot{\gamma}(t), \dot{\gamma}(t) \rangle = -2\langle \ddot{\gamma}(t), \gamma(t) \rangle - \frac{d}{dt} \langle \dot{\gamma}(t), \dot{\gamma}(t) \rangle = -2\langle \ddot{\gamma}(t), \gamma(t) \rangle,$$

$$h''''(t) = -2\langle \ddot{\gamma}(t), \gamma(t) \rangle - 2\langle \ddot{\gamma}(t), \dot{\gamma}(t) \rangle = -2\langle \ddot{\gamma}(t), \gamma(t) \rangle + 2\langle \ddot{\gamma}(t), \ddot{\gamma}(t) \rangle.$$

In the above, the last expression for the fourth derivative follows from the following computation:

$$0 = \frac{d^2}{dt^2} \langle \dot{\gamma}(t), \dot{\gamma}(t) \rangle = 2 \frac{d}{dt} \langle \ddot{\gamma}(t), \dot{\gamma}(t) \rangle = 2\langle \ddot{\gamma}(t), \dot{\gamma}(t) \rangle + 2\langle \ddot{\gamma}(t), \ddot{\gamma}(t) \rangle.$$

Now, at $t = 0$ we have:

$$h(0) = 0, \quad h'(0) = 0, \quad h''(0) = 0, \quad h'''(0) = 0, \quad h''''(0) = 2\langle \ddot{\gamma}(0), \ddot{\gamma}(0) \rangle,$$

since we have assumed $\gamma(0) = 0$. A Taylor expansion then shows that

$$h(t) = \frac{1}{12} \langle \ddot{\gamma}(0), \ddot{\gamma}(0) \rangle t^4 + O(t^5).$$

Hence

$$\begin{aligned} t &= |\gamma(t)| \sqrt{1 + \frac{1}{12} \langle \ddot{\gamma}(0), \ddot{\gamma}(0) \rangle \frac{t^4}{|\gamma(t)|^2} + \frac{1}{|\gamma(t)|^2} O(t^5)} \\ &= |\gamma(t)| \left(1 + \frac{1}{24} \langle \ddot{\gamma}(0), \ddot{\gamma}(0) \rangle \frac{t^4}{|\gamma(t)|^2} + \frac{1}{|\gamma(t)|^2} O(t^5) \right) \\ &= |\gamma(t)| + \frac{1}{24} \langle \ddot{\gamma}(0), \ddot{\gamma}(0) \rangle t^3 + O(t^4). \end{aligned}$$

The above shows that:

$$d_{\mathcal{M}}(x, y) = |x - y| + \frac{1}{24} \langle \ddot{\gamma}(0), \ddot{\gamma}(0) \rangle |x - y|^3 + O(|x - y|^4), \quad x, y \in \mathcal{M},$$

where in the above we interpret $\ddot{\gamma}(0)$ as the acceleration (in the ambient space) at time 0 of the unit speed geodesic going from x to y . The estimation of the term $\langle \ddot{\gamma}(0), \ddot{\gamma}(0) \rangle$ can be done through the estimation of the second fundamental form of \mathcal{M} , as indeed one can write

$$\ddot{\gamma}(0) = \mathbb{I}_x(\dot{\gamma}(0), \dot{\gamma}(0)).$$

The above discussion thus motivates introducing the function

$$\hat{d}_g(x, y) = |x - y| + \frac{1}{48} \left(|\hat{\mathbb{I}}_{xy}|^2 + |\hat{\mathbb{I}}_{yx}|^2 \right) |x - y|^3, \quad x, y \in \mathcal{X}, \quad (18)$$

where $\hat{\mathbb{I}}_{xy}$ is an estimator, built from data, for

$$\mathbb{I}_{xy} := \mathbb{I}_x(\dot{\gamma}(0), \dot{\gamma}(0)) = \mathbb{I}_x \left(\frac{\log_x(y)}{|\log_x(y)|}, \frac{\log_x(y)}{|\log_x(y)|} \right).$$

In section 3.2 we discuss some existing approaches in the literature for building these estimators. The relevant observation is that if $|\mathbb{I}_{xy}|^2$ can be approximated using $|\hat{\mathbb{I}}_{xy}|^2$ within error β , and using the fact that $|\mathbb{I}_{xy}|^2 = |\mathbb{I}_{yx}|^2 + O(|x - y|)$ given that the manifold \mathcal{M} is smooth, we would conclude that

$$|\hat{d}_g(x, y) - d_{\mathcal{M}}(x, y)| \leq C_1 \beta |x - y|^3 + C_2 |x - y|^4.$$

On the other hand, if \hat{d}_g had simply been defined as the Euclidean distance, the error of approximation of $d_{\mathcal{M}}$ would have been $O(|x - y|^3)$, as mentioned in Remark 3.

Remark 4. Notice that \hat{d}_g as in definition (18) is symmetric.

3.2 Quantitative estimates of second fundamental form from data

In this section we review some related literature on estimating the second fundamental form. Kim et al. [28] propose an estimator for the second fundamental form for embedded submanifolds, which is the class of manifolds considered in this paper. Specifically, they suggest to construct an estimator of the Hessian $H_h|_x$ of the defining function h at each point $x \in \mathcal{X}$ (recall Definition 1). To do this, they fit a quadratic polynomial p_h to the defining function in a small neighborhood of x and assume $H_{p_h}|_x \approx H_h|_x$. They show that such an approximation converges indeed asymptotically to the second fundamental form:

Theorem 5 ([28]). *Let the coefficients \tilde{A}_x of the polynomial p_h be determined by solving the weighted least-squares problem*

$$\tilde{A}_x = \operatorname{argmin}_Q \|K_x(XQ - h)\| \approx A_x ,$$

where X is the matrix of second-order monomials of points in \mathcal{X} centered at x ,

$$A_x = \frac{1}{2} \left[[H_h|_x]_{1,1}, [H_h|_x]_{1,2}, \dots, [H_h|_x]_{d,d} \right]^T$$

$$\tilde{A}_x = \frac{1}{2} \left[[H_{p_h}|_x]_{1,1}, [H_{p_h}|_x]_{1,2}, \dots, [H_{p_h}|_x]_{d,d} \right]^T ,$$

and K_x a diagonal matrix with $\operatorname{diag}(K_x) = \mathbf{1}_{\|x_i - x\| \leq \varepsilon}$. Then $\|A_x - \tilde{A}_x\| \rightarrow 0$ for all $x \in \mathcal{X}$ as $n \rightarrow \infty, \varepsilon \rightarrow 0$.

A proof can be found in [28, Appendix, (sections 1-2)].

While this result holds for any manifold considered in this paper, it provides only *asymptotic* guarantees. Aamari and Levrard [1] show that under additional smoothness assumptions on the underlying manifold, one can indeed obtain non-asymptotic error estimates. They give minimax bounds of order $O\left(n^{\frac{2-k}{m}}\right)$ [1, Theorems 4 and 5] for an estimator of the second fundamental form of a C^k -smooth embedded submanifold. Below, we briefly recall the minimax bounds for later reference. To state the results, we introduce the following additional notation. We define, as usual, the *operator norm* of a linear map T on $S \subset \mathbb{R}^d$ as $\|T\|_{op} := \sup_{z \in S} \frac{\|Tz\|}{\|z\|}$. Let \mathcal{M} be a C^k -manifold with $k \geq 3$ and reach $\tau \geq \tau_{\min} > 0$. For $x \in \mathcal{X}$, one can define the local estimator

$$(\hat{\pi}_j, \hat{T}_{2,j}, \dots, \hat{T}_{k-1,j}) \in \operatorname{argmin}_{\pi, \sup_{2 < i < k} \|T_i\|_{op} \leq 1} P_{n-1}^{(j)} \left[\left\| x - \pi(x) - \sum_{i=2}^{k-1} T_i(\pi(x)^{\otimes i}) \right\|^2 \mathbf{1}_{B(0,h)}(x) \right] , \quad (19)$$

where π is an orthogonal projection onto d -dimensional subspaces and $T_i : (\mathbb{R}^m)^i \rightarrow \mathbb{R}^m$ a bounded symmetric tensor of order i . Moreover, $P_{n-1}^{(j)}$ denotes integration with respect to $\frac{1}{(n-1)} \sum_{i \neq j} \delta_{(x_i - x_j)}$, $z^{\otimes i}$ the $(m \times i)$ -dimensional vector (z, \dots, z) and $h \leq \frac{\tau_{\min}}{8}$. Aamari and Levrard give the following guarantee for a solution of Eq. 19:

Theorem 6 ([1]). *Let \mathcal{M} be a C^k -manifold with $k \geq 3$ and reach $\tau \geq \tau_{\min} > 0$. For sufficiently large n , we have with probability at least $1 - (\frac{1}{n})^{k/d}$:*

1. *Upper bound:*

$$\mathbb{E} \left[\max_{1 \leq j \leq n} \|\mathbb{I}_{x_j y} \circ \pi_{T_{x_j} \mathcal{M}} - \hat{T}_{2,j} \circ \hat{\pi}_j\|_{op} \right] \leq C \left(\frac{\log n}{n-1} \right)^{\frac{k-2}{d}} \quad (20)$$

2. *Lower bound:*

$$\inf \mathbb{E} \left[\|\mathbb{I}_{x_j y} \circ \pi_{T_{x_j} \mathcal{M}} - \hat{T}_{2,j} \circ \hat{\pi}_j\|_{op} \right] \geq C' \left(\frac{1}{n-1} \right)^{\frac{k-2}{d}} \quad (21)$$

Here, C, C' are constants depending on d, k, τ_{\min} ; n is assumed to be sufficiently large, such that $C^{-1} \geq (\sup_{2 \leq i \leq k} \|T_i^*\|_{op})^{-1}$ for the estimator.

It should be noted that Eq. 19 can be difficult to solve in practise, with one approach viewing Eq. 19 as an optimization task on the Grassman manifold [44]. We further note that similar estimation results were also obtained in related work by Cao et al. [10].

Notice that Theorem 6 provides *error bounds* in expectation, which do not immediately translate into concentration bounds. While a development of such concentration bounds is beyond the scope of the present paper, we briefly comment on a possible avenue for deriving them, at least in the large-sample regime. Specifically, given a sufficiently large sample, one may construct approximations of tangent spaces via principal component analysis. Developing a means to track the change in the tangent space as we move along the manifold could deliver an approximation of the second fundamental form, which, in turn, would allow for deriving concentration bounds.

3.3 Geodesic distances on \mathcal{X}

To define a geodesic distance d_G over $G = (\mathcal{X}, w_\varepsilon)$ (interpreting w_ε as either (10) or as (11)) we first introduce the following “pre-distance” functions:

$$\tilde{d}_{G, \mathcal{M}}(x, y) := \begin{cases} 0, & \text{if } x = y, \\ \delta_0 \psi \left(\frac{d_{\mathcal{M}}(x, y)}{\delta_0} \right), & \text{if } 0 < d_{\mathcal{M}}(x, y) \leq \delta_1, \\ +\infty, & \text{otherwise,} \end{cases}$$

and

$$\tilde{d}_{G, \mathcal{X}}(x, y) := \begin{cases} 0, & \text{if } x = y, \\ \delta_0 \psi \left(\frac{\hat{d}_g(x, y)}{\delta_0} \right), & \text{if } 0 < \hat{d}_g(x, y) \leq \delta_1, \\ +\infty, & \text{otherwise,} \end{cases}$$

where \hat{d}_g satisfies Assumption 1. In the above, we use parameters $\delta_0 < \delta_1$ that in terms of the parameter ε will be written as

$$\delta_0 := c_0 \varepsilon, \quad \delta_1 := c_1 \varepsilon \quad (22)$$

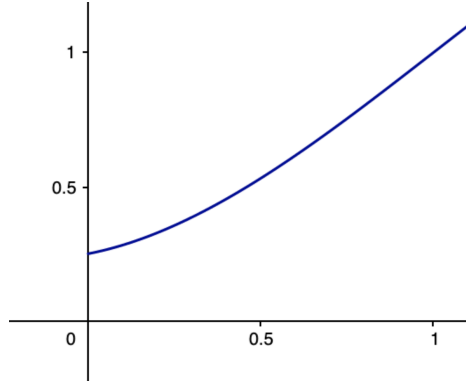


Figure 2: Plot of the function $\psi(t) := \begin{cases} \frac{1}{4}(1-t)^3 + t & \text{if } 0 \leq t \leq 1 \\ t & \text{if } t > 1 \end{cases}$, which satisfies all the required conditions in Assumption 2.

where c_0 is a fixed but small enough number and c_1 is fixed but large enough; see more details below. Finally, the profile function ψ appearing in both definitions is assumed to satisfy the following conditions:

Assumption 2. *The function $\psi : [0, \infty) \rightarrow [0, \infty)$ satisfies the following:*

1. ψ is C^2 , non-decreasing, and convex.
2. $\psi(t) = t$ for all $t \geq 1$.
3. $\psi(0) > 0$ and $\psi'(0) > 0$.

In Figure 2 we provide an example of an admissible profile function ψ . As we discuss in detail in Remark 17, Assumption 2 guarantees that the geometry of the RGG is suitably glued together when moving from two lengthscales at which the RGG exhibits two different geometric behaviors.

We may now use the above pre-distance functions to define two geodesic distances over \mathcal{X} :

$$d_{G,\mathcal{M}}(x, y) := \inf_{\substack{n \in \mathbb{N}, \{x_i\}_{i=0}^n \subseteq \mathcal{X} \\ x_0=x, x_n=y}} \sum_{i=0}^{n-1} \tilde{d}_{G,\mathcal{M}}(x_i, x_{i+1}), \quad (23)$$

and

$$d_{G,\mathcal{X}}(x, y) := \inf_{\substack{n \in \mathbb{N}, \{x_i\}_{i=0}^n \subseteq \mathcal{X} \\ x_0=x, x_n=y}} \sum_{i=0}^{n-1} \tilde{d}_{G,\mathcal{X}}(x_i, x_{i+1}). \quad (24)$$

Note that, in contrast to $d_{G,\mathcal{M}}$, the function $d_{G,\mathcal{X}}$ is completely data-driven and thus in principle more useful in applications, unless $d_{\mathcal{M}}$ is known, in which case one could directly work with $d_{G,\mathcal{M}}$. Either way, as we show below, both $d_{G,\mathcal{M}}$

and $d_{G,\mathcal{X}}$ are indeed distance functions over \mathcal{X} and both of them induce Olivier Ricci curvature functions that recover \mathcal{M} 's Ricci curvature in the large data limit.

Lemma 1. *Let $d_G = d_{G,\mathcal{M}}$ and $\tilde{d}_G = \tilde{d}_{G,\mathcal{M}}$, or $d_G = d_{G,\mathcal{X}}$ and $\tilde{d}_G = \tilde{d}_{G,\mathcal{X}}$. In either case the function d_G is a distance over \mathcal{X} . Moreover, for every $x, y \in \mathcal{X}$ there exists a finite sequence $x_1, \dots, x_k \in \mathcal{X}$ such that:*

1. $x_1 = x$, and $x_k = y$.
2. $d_G(x_i, x_{i+1}) = \tilde{d}_G(x_i, x_{i+1}) \leq \delta_1$.
3. $d_G(x, y) = \sum_{i=1}^{k-1} d_G(x_i, x_{i+1})$.

Proof. The fact that $d_G = d_{G,\mathcal{M}}$ is a distance function follows directly from the definitions. Likewise, we can see that $d_G = d_{G,\mathcal{X}}$ is a distance function thanks to the fact that \hat{d}_g is symmetric, according to Assumption 1.

To prove the second part, notice that for an arbitrary pair $x, y \in \mathcal{X}$ we can find a path $x_1, \dots, x_k \in \mathcal{X}$ with $x_1 = x$ and $x_k = y$ such that $d_G(x, y) = \sum_{i=1}^{k-1} \tilde{d}_G(x_i, x_{i+1})$. Now, by definition of $d_G(x_i, x_{i+1})$, we have $\tilde{d}_G(x_i, x_{i+1}) \geq d_G(x_i, x_{i+1})$ for every $i = 1, \dots, k-1$. If the inequality was strict for at least one i , then we would actually be able to build a path connecting x, y whose length is strictly smaller than $d_G(x, y)$, which would be a contradiction. It follows that $d_G(x_i, x_{i+1}) = \tilde{d}_G(x_i, x_{i+1})$ for all $i = 1, \dots, k-1$. □

Lemma 2. *Let $\kappa \in \mathbb{R}$ and suppose that*

$$1 - \frac{W_{1,G}(\mu_x^G, \mu_y^G)}{d_G(x, y)} \geq \kappa, \quad (25)$$

for every $x, y \in \mathcal{X}$ satisfying $d_G(x, y) = \tilde{d}_G(x, y) \leq \delta_1$. Then (25) holds for any pair $x, y \in \mathcal{X}$

Proof. Thanks to Lemma 1, the proof is just as in [Prop. 19, [36]]. The emphasis here, however, is the fact that we only need to check the inequality for pairs x, y for which the distance function d_G and the pre-distance function \tilde{d}_G coincide. □

We finish this section with the following inequalities relating the metrics $d_{G,\mathcal{X}}$, $d_{G,\mathcal{M}}$, and $d_{\mathcal{M}}$. These inequalities will only be used later on in section 6.3 when studying curvature upper bounds.

Proposition 2. *Under Assumption 1, for all small enough ε and β the following holds:*

$$d_{G,\mathcal{M}}(x, y) \geq d_{\mathcal{M}}(x, y), \quad (26)$$

for all $x, y \in \mathcal{X}$, and, with probability at least $1 - C \exp(-\zeta(n, \beta, \varepsilon))$ we have

$$(1 + C(\beta\varepsilon^2 + \varepsilon^3))d_{G,\mathcal{X}}(x, y) \geq d_{\mathcal{M}}(x, y). \quad (27)$$

for all $x, y \in \mathcal{X}$. Moreover, if $x, y \in \mathcal{X}$ are such that $2\delta_0 \leq d_{\mathcal{M}}(x, y) \leq \frac{1}{2}\delta_1$, where δ_0 and δ_1 are as in the definition of $d_{G, \mathcal{X}}$ and $d_{G, \mathcal{M}}$, then

$$d_{G, \mathcal{X}}(x, y) \leq d_{\mathcal{M}}(x, y)(1 + C(\beta\varepsilon^2 + \varepsilon^3)) \quad (28)$$

and

$$d_{G, \mathcal{M}}(x, y) \leq d_{\mathcal{M}}(x, y). \quad (29)$$

Proof. Inequality (26) is immediate from the triangle inequality for $d_{\mathcal{M}}$ and the fact that $\tilde{d}_{G, \mathcal{M}}(x_i, x_{i+1}) \geq \delta_0\psi(d_{\mathcal{M}}(x_i, x_{i+1})/\delta_0) \geq d_{\mathcal{M}}(x_i, x_{i+1})$ for any two data points x_i, x_{i+1} with $d_{\mathcal{M}}(x_i, x_{i+1}) \leq \delta_1$, since necessarily $\psi(t) \geq t$ for all $t \geq 0$.

To prove inequality (27), consider an arbitrary discrete path $\{x_i\}_{i=0}^n$ connecting x and y such that $\tilde{d}_{G, \mathcal{X}}(x_i, x_{i+1}) < \infty$ for all i . Then

$$\begin{aligned} \sum_{i=0}^{n-1} \tilde{d}_{G, \mathcal{X}}(x_i, x_{i+1}) &= \sum_{i=0}^{n-1} \delta_0\psi(\hat{d}_g(x_i, x_{i+1})/\delta_0) \\ &= \sum_{i \in A} \delta_0\psi(\hat{d}_g(x_i, x_{i+1})/\delta_0) + \sum_{i \in B} \delta_0\psi(\hat{d}_g(x_i, x_{i+1})/\delta_0) \\ &\geq \sum_{i \in A} \hat{d}_g(x_i, x_{i+1}) + \sum_{i \in B} \delta_0\psi(\hat{d}_g(x_i, x_{i+1})/\delta_0), \end{aligned}$$

where $A := \{i \text{ s.t. } \hat{d}_g(x_i, x_{i+1}) \leq \frac{3}{4}\psi(0)\delta_0\}$ and $B := \{i \text{ s.t. } \hat{d}_g(x_i, x_{i+1}) > \frac{3}{4}\psi(0)\delta_0\}$. For an $i \in A$, we can use 2 in Assumption 1 to conclude that $d_{\mathcal{M}}(x, y) \leq \delta_0\psi(0) \leq \tilde{d}_{G, \mathcal{X}}(x_i, x_{i+1})$, whereas for an i in B we can use 1 in Assumption 1 to bound the difference between $\hat{d}_g(x_i, x_{i+1})$ and $d_{\mathcal{M}}(x_i, x_{i+1})$. In particular,

$$\begin{aligned} \sum_{i=0}^{n-1} \tilde{d}_{G, \mathcal{X}}(x_i, x_{i+1}) &\geq \sum_{i \in A} (\hat{d}_g(x_i, x_{i+1}) - d_{\mathcal{M}}(x_i, x_{i+1}) + d_{\mathcal{M}}(x_i, x_{i+1})) \\ &\quad + \sum_{i \in B} d_{\mathcal{M}}(x_i, x_{i+1}) \\ &\geq \sum_{i=0}^{n-1} (1 - C_1\beta\varepsilon^2 - C_2\varepsilon^3)d_{\mathcal{M}}(x_i, x_{i+1}) \\ &\geq (1 - C_1\beta\varepsilon^2 - C_2\varepsilon^3)d_{\mathcal{M}}(x, y), \end{aligned}$$

where the last inequality follows from the triangle inequality for $d_{\mathcal{M}}$. From this we deduce that

$$(1 + C(\beta\varepsilon^2 + \varepsilon^3))d_{G, \mathcal{X}}(x, y) \geq d_{\mathcal{M}}(x, y),$$

for some constant C .

To prove (28), notice that, under the assumption that ε is small enough, we can guarantee, thanks to (16), that $\hat{d}_g(x, y) \in [\delta_0, \delta_1]$. This means that

$$d_{G, \mathcal{X}}(x, y) \leq \hat{d}_g(x, y).$$

In turn, applying (16) again we can upper bound $\hat{d}_g(x, y)$ from above by $(1 + C(\beta\varepsilon^2 + \varepsilon^3))d_{\mathcal{M}}(x, y)$. Inequality (28) now follows.

Inequality (29) is obvious from the definition of $d_{G, \mathcal{M}}$ and the assumption on $d_{\mathcal{M}}(x, y)$. □

4 Main results

We are now ready to state our main results. Throughout this section we will make the following assumptions on the scale of the parameters that determine G , the estimator d_g , and the discrete curvature κ_G .

Assumption 3. *We assume that the following relations hold:*

1. $c_1 \geq 2 + 4c_0$, where c_0 and c_1 are as in (22).
2. ε and β are sufficiently small and n is sufficiently large.
3. The ratio $\frac{\log(n)^{p_m}}{n^{1/m}\varepsilon^3}$ is sufficiently small, where p_m is a dimension dependent quantity: $p_m = 3/4$ when $m = 2$, and $p_m = 1/m$ when $m \geq 3$.

4.1 Pointwise Consistency

Van der Hoorn et al. [45] were the first to analyze the *pointwise consistency* of some form of discrete Ricci curvature on an RGG. They give *asymptotic* convergence guarantees of the following form:

Proposition 1 (Pointwise consistency [45]). *Let $\langle \cdot \rangle$ denote the expectation with respect to the RGG ensemble $G = (\mathcal{X}, w_{\varepsilon, \mathcal{M}})$. Suppose that d_G is taken to be $d_{\mathcal{M}}$ in (14). Finally, suppose that $\varepsilon = \varepsilon_n \sim n^{-\alpha}$ and $\delta = \delta_n = n^{-\beta}$ with $0 < \beta \leq \alpha$ and $\alpha + 2\beta < \frac{1}{m}$.*

Then

$$\lim_{n \rightarrow \infty} \left\langle \left| \frac{1}{\delta^2} \kappa_G - \frac{1}{2(m+2)} \text{Ric}_x(v) \right| \right\rangle = 0, \quad (30)$$

where $y = y_n$ is the point on the geodesic in direction v starting at x with $\delta = d_{\mathcal{M}}(x, y)$.

Remark 7. *It is worth pointing out that in the definition of κ_G in [45] we have $d_G = d_{\mathcal{M}}$, where as here where we work with $d_{G, \mathcal{M}}$. When working with $d_{G, \mathcal{M}}$ we will be able to obtain global lower bounds for our induced curvature, while those lower bounds can not be derived for $d_{\mathcal{M}}$.*

The authors of [45] provide a second analysis which only requires access to pairwise Euclidean distances in the ambient space, but this result relies on a crucial auxiliary result, which is currently only available in dimension 2.

In what follows we address Problem 1 and provide *non-asymptotic* error bounds for the approximation of \mathcal{M} 's Ricci curvature from our notions of discrete Ricci curvature. Our first result is stated in the setting where we have access to $d_{\mathcal{M}}$.

Theorem 8. *Let \mathcal{M} be an m -dimensional, compact, boundaryless, connected, smooth manifold embedded in \mathbb{R}^d . Let $\mathcal{X} = \{x_1, \dots, x_n\}$ consist of i.i.d. samples from the uniform distribution on \mathcal{M} . Let $w_\varepsilon = w_{\varepsilon, \mathcal{M}}$ be defined according to (10), let $d_G = d_{G, \mathcal{M}}$ be the metric defined in (23) for a profile function ψ satisfying Assumptions 2, and let κ_G be the Ollivier Ricci curvature induced by these choices of Ollivier balls and metric (see (14)).*

Under Assumption 3, for every $s > 1$ there is a constant C such that, with probability at least $1 - Cn^{-s}$, we have

$$\left| \frac{\kappa_G(x, y)}{\varepsilon^2} - \frac{\text{Ric}_x(v)}{2(m+2)} \right| \leq C \left(\varepsilon + \frac{\log(n)^{p_m}}{n^{1/m} \varepsilon^3} \right), \quad (31)$$

for all $x, y \in \mathcal{X}$ satisfying $2\delta_0 \leq d_{\mathcal{M}}(x, y) \leq \frac{1}{2}\delta_1$, where δ_0 and δ_1 are defined in (22). In the above, we use v to denote the vector $\frac{\log_x(y)}{|\log_x(y)|} \in T_x \mathcal{M}$, and $p_m = 3/4$ if $m = 2$, while $p_m = 1/m$ if $m \geq 3$

A second result, which only assumes access to a sufficiently sharp data-driven approximation of the geodesic distance $d_{\mathcal{M}}$, is stated below.

Theorem 9 (Pointwise consistency 2). *Let \mathcal{M} be an m -dimensional, compact, boundaryless, connected, smooth manifold embedded in \mathbb{R}^d . Let $\mathcal{X} = \{x_1, \dots, x_n\}$ consist of i.i.d. samples from the uniform distribution on \mathcal{M} . Let $w_\varepsilon = w_{\varepsilon, \mathcal{X}}$ be defined according to (11), for a data-driven approximation \hat{d}_g of $d_{\mathcal{M}}$ satisfying Assumption 1. Let $d_G = d_{G, \mathcal{X}}$ be the metric defined in (24) for a profile function ψ satisfying Assumptions 2, and let κ_G be the Ollivier Ricci curvature induced by these choices of Ollivier balls and metric (see (14)).*

Under Assumption 3, for every $s > 1$ there is a constant C such that, with probability at least $1 - Cn^{-s} - C \exp(-\zeta(n, \beta, \varepsilon))$, we have

$$\left| \frac{\kappa_G(x, y)}{\varepsilon^2} - \frac{\text{Ric}_x(v)}{2(m+2)} \right| \leq C \left(\beta + \varepsilon + \frac{\log(n)^{p_m}}{n^{1/m} \varepsilon^3} \right), \quad (32)$$

for all $x, y \in \mathcal{X}$ satisfying $3\delta_0 \leq \hat{d}_g(x, y) \leq \frac{1}{3}\delta_1$. The quantities δ_0 , δ_1 , v and p_m are as in Theorem 8.

4.2 Global Curvature Lower Bounds

We turn our attention to Problem 2 and state two theorems relating global lower bounds for Ric and κ_G . In section 7, we complement our analysis with a discussion of applications of the curvature lower bounds stated below.

In our first result we assume access to the geodesic distance $d_{\mathcal{M}}$.

Theorem 10 (Global lower bounds). *Let \mathcal{M} be an m -dimensional, compact, boundaryless, connected, smooth manifold embedded in \mathbb{R}^d with Ricci curvature lower bounded by $2(m+2)K$. Let $\mathcal{X} = \{x_1, \dots, x_n\}$ consist of i.i.d. samples from the uniform distribution on \mathcal{M} . Let $w_\varepsilon = w_{\varepsilon, \mathcal{M}}$ be defined according to (10), let $d_G = d_{G, \mathcal{M}}$ be the metric defined in (23) for a profile function ψ satisfying Assumptions 2, and let κ_G be the Ollivier Ricci curvature induced by these choices of Ollivier balls and metric (see (14)).*

Under Assumption 3, for every $s > 1$ there is a constant C such that, with probability at least $1 - Cn^{-s}$, we have

$$\frac{\kappa_G(x, y)}{\varepsilon^2} \geq \min \left\{ s_K K - C \left(\varepsilon + \frac{\log(n)^{p_m}}{n^{1/m} \varepsilon^3} \right), \frac{1}{2\varepsilon^2} \right\}, \quad \forall x, y \in \mathcal{X}, \quad (33)$$

where the factor s_K is given by

$$s_K := \begin{cases} \frac{\psi'(0)c_0}{12c_1 C_{\mathcal{M}}} & \text{if } K \geq 0 \\ \frac{c_1}{c_0 \psi(0)} & \text{if } K < 0, \end{cases}$$

where c_0, c_1 are as in (22), and $C_{\mathcal{M}}$ is a manifold dependent constant that in particular implies $\frac{c_0}{12c_1 C_{\mathcal{M}}} \leq 1$. Also, $p_m = 3/4$ if $m = 2$, while $p_m = 1/m$ if $m \geq 3$.

Remark 11. *The rescaling of κ_G by ε^2 is the right scaling when passing to the continuum limit, i.e. $n \rightarrow \infty$ and $\varepsilon \rightarrow 0$. This can already be seen from our pointwise consistency results in section 4.1, but it can also be interpreted as a way to properly rescale the time variable indexing the discrete-time random walk on G . In particular, we will see in section 7.1 that (33) implies novel contraction properties for the heat flow (continuous time) on G when we assume the manifold \mathcal{M} to be positively curved.*

Remark 12. *The factor s_K makes the lower bound in (33) looser than the lower bound for \mathcal{M} 's Ricci curvature: when $K \geq 0$, s_K is necessarily smaller than one (but still strictly positive, since $\psi'(0) > 0$), whereas when $K < 0$ the quantity s_K is greater than one. The appearance of s_K is due to the fact that in our analysis we must glue together two estimates that hold at different length-scales, and, in doing so, we end up with a suboptimal bound. Presumably, our analysis can be sharpened, but this aim is out of the scope of this paper.*

A second result, which only assumes access to a sufficiently sharp data-driven approximation of the geodesic distance $d_{\mathcal{M}}$, is stated below.

Theorem 13 (Consistency of global bounds 2). *Let \mathcal{M} be an m -dimensional, compact, boundaryless, connected, smooth manifold embedded in \mathbb{R}^d with Ricci curvature lower bounded by $2(m+2)K$. Let $\mathcal{X} = \{x_1, \dots, x_n\}$ consist of i.i.d. samples from the uniform distribution on \mathcal{M} . Let $w_\varepsilon = w_{\varepsilon, \mathcal{X}}$ be defined according to (11), for a data-driven approximation \hat{d}_g of $d_{\mathcal{M}}$ satisfying Assumption*

1. Let $d_G = d_{G,\mathcal{X}}$ be the metric defined in (24) for a profile function ψ satisfying Assumptions 2, and let κ_G be the Ollivier Ricci curvature induced by these choices of Ollivier balls and metric (see (14)).

Under Assumption 3, for every $s > 1$ there is a constant C such that, with probability at least $1 - Cn^{-s} - C \exp(-\zeta(n, \beta, \varepsilon))$, we have

$$\frac{\kappa_G(x, y)}{\varepsilon^2} \geq \min \left\{ s_K K - C \left(\varepsilon + \beta + \frac{\log(n)^{p_m}}{n^{1/m} \varepsilon^3} \right), \frac{1}{4\varepsilon^2} \right\}, \quad \forall x, y \in \mathcal{X}, \quad (34)$$

where the factor s_K is as in Theorem 10, and $p_m = 3/4$ if $m = 2$, while $p_m = 1/m$ if $m \geq 3$.

As we will discuss in section 7.1, the above curvature lower bounds provide information on the behavior of Lipschitz seminorms along the heat flow induced by the graph Laplacian associated to the RGG $G = (\mathcal{X}, w_\varepsilon)$.

4.3 Numerical examples

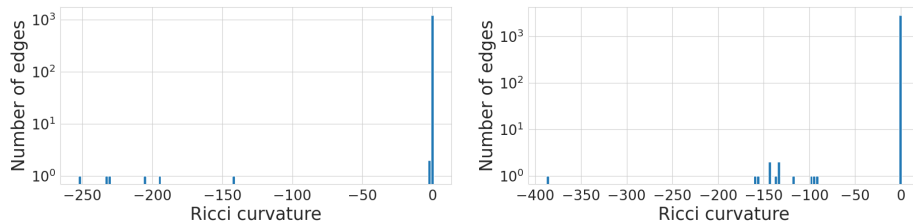
We illustrate the recovery of global lower bounds (Theorem 10) on the example of a unit d -sphere. Since the unit d -sphere has sectional curvature 1, we expect to recover a global lower bound of 1 for Ollivier's Ricci curvature in a random geometric graph, in the large-sample limit. To test this numerically, we sample n points uniformly at random from the unit d -sphere, centered at the origin. Sampling is performed via sphere picking (also known as Muller-Marsaglia algorithm [32]): We sample d independent random variables from the standard normal distribution $z = (z_1, \dots, z_d)$. The point $(\sum_i z_i)^{-1/2} z$ lies on the unit d -sphere. We repeat this procedure n times to generate a sample of size n . Figure 3 shows the curvature distribution of the resulting random geometric graphs with different hyperparameters. We see that almost all edges have indeed a Ricci curvature of 1, as predicted by our theoretical results¹.

In our numerical experiments, the 1-Wasserstein distance is computed via the Hungarian algorithm, which has a cubic complexity. Hence, for large sample sizes it is expensive to compute Ollivier's curvature on each edge in the RGG. However, as a byproduct of our global lower curvature bounds, we develop upper and lower bounds on the 1-Wasserstein distance, which do not require optimizing transport maps, but can be computed from combinatorial arguments. Thus, in applications in which we mainly rely on global lower curvature bounds (see examples in the next section), our approach nevertheless allows for an efficient characterization of the manifolds's geometry.

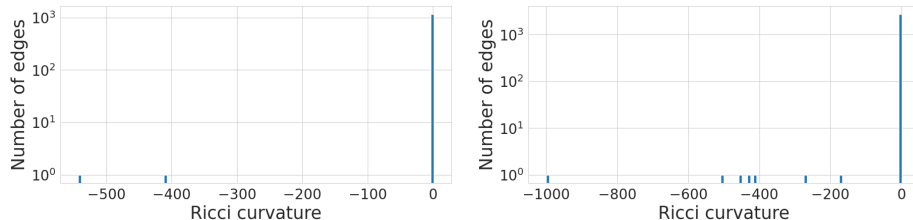
5 Related Work

Throughout this work, we consider Ricci curvature in the sense of Ollivier [36, 37]. Our analysis utilizes several theoretical results that date back to Ollivier's

¹The small number of outliers are due to numerical inaccuracies, specifically, (1) the sample distribution is not perfectly uniform and (2) some sample points do not lie exactly on the sphere.



(a) Sample size $n = 500$ (left) and $n = 750$ (right) with parameters $\varepsilon = 0.2, \delta_0 = 0.01, \delta_1 = 0.02$.



(b) Sample size $n = 1000$ (left) and $n = 1500$ (right) with parameters $\varepsilon = 0.1, \delta_0 = 0.005, \delta_1 = 0.01$

Figure 3: Distribution of curvature values for a random geometric graph G_ε constructed from n data points sampled from the 2-sphere $\mathbb{S}^2 \subseteq \mathbb{R}^3$. The vertical axis is plotted in log-scale.

work [36]. As mentioned above, the pointwise consistency of Ollivier’s Ricci curvature between RGGs and an underlying manifolds has been previously studied in [45], which gave *asymptotic* guarantees assuming access to geodesic distances, and also when not having access to geodesic distances, but only in a very special case.

Other popular discrete Ricci curvatures include notions by Forman [20] and Maas and Erbar [16], as well as a notion by Lin-Yau [29], which is closely related to Ollivier’s Ricci curvature. The relation between Forman’s Ricci curvature and that of an underlying manifold has recently been explored in [31]. Notably, Maas and Erbar’s Ricci curvature allows for a log-Sobolev inequality (via a discrete Bakry-Emery theorem) and the inference of curvature lower bounds [18], although not in a tractable way that would allow one to infer its consistency in the RGG setting. Discrete Ricci curvatures have been related to a range of classical graph characteristics [27, 49, 50] and have found applications in network analysis and machine learning [17, 19, 35, 40, 43, 48, 52]. Beyond [45], to the best of our knowledge there is no other work rigorously connecting the discrete Ricci curvature of a point cloud and the Ricci curvature of a manifold.

Continuum limits of different geometric characteristics defined on data clouds have been explored in the literature. For example, the analysis of graph Laplacians and their convergence toward Laplace-Beltrami operators on manifolds has received a lot of attention in the last decades, e.g., in [24, 41] where point-

wise consistency results are presented, and in [6, 8, 9, 15, 22, 51], where spectral consistency is discussed.

Other works explore the discrete-to-continuum convergence of general data-driven distances, e.g., see [5, 12, 13, 25, 26, 30] and some of the references therein. The papers [5, 12, 13], for example, discuss convergence of distances defined on random geometric graphs (RGG), either in the i.i.d. setting or for Poisson point processes. The results from [12] are asymptotic, while the ones in [5, 13] provide high probability convergence rates in terms of an RGG's connectivity parameter. The results in [5], for example, discuss the convergence of the ratio between certain expectations of distances at different scales. When combined with concentration inequalities, this allows the authors to prove rates of convergence, in sparse settings, for a semisupervised learning procedure known as Lipschitz learning; see [5, 38]. Finally, [7] presents a graph-PDE approach to approximate geodesic distances by analyzing variants of the Eikonal equation on a graph. Many of the approaches discussed in the aforementioned papers could potentially be used to define estimators \hat{d}_g for $d_{\mathcal{M}}$.

The approach for estimating $d_{\mathcal{M}}$ from data outlined in section 3 relies on the approximation of the second fundamental form from data. Some papers that explore the estimation of the second fundamental form are [1, 10, 28].

6 Nonasymptotic Guarantees on Curvature Consistency

In this section we present proofs for our main results. After some preliminary discussion, we first show the consistency of global curvature bounds, followed by a proof of pointwise, local consistency. A summary of the notation used throughout this section can be found in Table 1.

6.1 Preliminaries

In this subsection we collect a series of preliminary results and estimates that we use in the proofs of our main results.

6.1.1 Some lemmas from optimal transport theory

We recall the Kantorovich-Rubinstein duality theorem for the 1-Wasserstein metric between two probability measures over the same Polish metric space.

Theorem 14 (Kantorovich-Rubinstein, cf. Thm 1.14, [46]). *Let μ_1, μ_2 be two (Borel) probability measures over a Polish metric space (\mathcal{U}, d) . Then*

$$W_1(\mu_1, \mu_2) := \sup_{f \text{ s.t. } \text{Lip}(f) \leq 1} \int f(\tilde{x}) d\mu_1(\tilde{x}) - \int f(\tilde{y}) d\mu_2(\tilde{y}).$$

In the above, $\text{Lip}(f)$ stands for the Lipschitz constant (relative to the metric d) of the function f .

$B(x, \varepsilon)$	Euclidean ball
$B_{\mathcal{M}}(x, \varepsilon)$	Ollivier ball, continuous setting
$B_G(x, \varepsilon)$	Ollivier ball, discrete setting
$d_{\mathcal{M}}(x, y)$	geodesic distance on \mathcal{M}
$\hat{d}_g(x, y)$	data-driven local approximation of $d_{\mathcal{M}}$
$\tilde{d}_{G, \mathcal{M}}(x, y)$	pre-distance on \mathcal{X} , access to distances on \mathcal{M} (Eq. 23)
$\tilde{d}_{G, \mathcal{X}}(x, y)$	pre-distance on \mathcal{X} , data-driven (Eq. 24)
$d_{G, \mathcal{M}}(x, y)$	distance on \mathcal{X} , access to distances on \mathcal{M} (Eq. 23)
$d_{G, \mathcal{X}}(x, y)$	distance on \mathcal{X} , data-driven (Eq. 24)
$K(u, v)$	sectional curvature (Eq. 2)
$\text{Ric}_x(v)$	Ricci curvature (Eq. 1)
$W_1(\mu, \nu)$	1-Wasserstein distance w.r.t. $d_{\mathcal{M}}$ or for a generic metric d (clear from context) (Eq. 4)
$W_{1,G}(\mu, \nu)$	1-Wasserstein distance w.r.t. d_G (Eq. 15)
$W_{\infty}(\mu, \nu)$	∞ -OT distance (Eq. 36)

Table 1: Summary of notation.

Next, we recall the notion of *glueing* of couplings. Given finite positive measures μ_1, \dots, μ_k over a Polish space (\mathcal{U}, d) , all of which have the same total mass, and given couplings $\pi_{12}, \pi_{23}, \dots, \pi_{k-1,k}$ with $\pi_{l,l+1} \in \Gamma(\mu_l, \mu_{l+1})$, we define Π , the glueing of the couplings $\pi_{l,l+1}$, as the measure over \mathcal{U}^k satisfying

$$\int \varphi(x_1, \dots, x_k) d\Pi(x_1, \dots, x_k) = \int \int \dots \int \varphi(x_1, \dots, x_k) d\pi_{k-1,k}(x_k|x_{k-1}) \dots d\pi_{1,2}(x_2|x_1) d\mu_1(x_1) \quad (35)$$

for all regular enough test functions φ ; in the above, $\pi_{l,l+1}(\cdot|x_l)$ must be interpreted as the conditional distribution of x_{l+1} given x_l when (x_l, x_{l+1}) are jointly distributed according to $\pi_{l,l+1}$. For given $l, s \in \{1, \dots, k\}$ consider the map $T_{l,s} : (x_1, \dots, x_k) \mapsto (x_s, x_l)$. It is straightforward to see that $T_{l,s}\#\Pi \in \Gamma(\mu_s, \mu_l)$.

Next, we present the following lemma.

Lemma 3. *Let $\mu_1, \mu_2, \tilde{\mu}_1, \tilde{\mu}_2$ be finite positive measures defined over the same Polish space (\mathcal{U}, d) , satisfying $\mu_1(\mathcal{U}) = \tilde{\mu}_1(\mathcal{U})$ and $\mu_2(\mathcal{U}) = \tilde{\mu}_2(\mathcal{U})$. Then*

$$W_1(\mu_1 + \mu_2, \tilde{\mu}_1 + \tilde{\mu}_2) \leq W_1(\mu_1, \tilde{\mu}_1) + W_1(\mu_2, \tilde{\mu}_2).$$

Proof. The desired inequality follows from the observation that for any two couplings $\pi_1 \in \Gamma(\mu_1, \tilde{\mu}_1)$ and $\pi_2 \in \Gamma(\mu_2, \tilde{\mu}_2)$ we have $\pi_1 + \pi_2 \in \Gamma(\mu_1 + \mu_2, \tilde{\mu}_1 + \tilde{\mu}_2)$. \square

6.1.2 Some estimates for the ∞ -OT distance between measures

In the proofs of our main results we will make use of the ∞ -OT distance $W_{\infty}(\cdot, \cdot)$ between probability measures defined over the same metric space. Precisely, let

μ_1, μ_2 be two (Borel) probability measures over a Polish metric space (\mathcal{U}, d) . We define $W_\infty(\mu_1, \mu_2)$ as

$$W_\infty(\mu_1, \mu_2) := \inf_{\pi \in \Gamma(\mu_1, \mu_2)} \sup_{(\tilde{x}, \tilde{y}) \in \text{spt}(\pi)} d(\tilde{x}, \tilde{y}), \quad (36)$$

where $\text{spt}(\pi)$ stands for the support of the measure π .

The following results relate, on the one hand, the ∞ -OT distance between two measures with densities with respect to the uniform measure over a Euclidean (or geodesic) ball, and on the other hand the L^∞ distance between the densities.

Proposition 3 (cf. Thm. 1.2, [23]). *Let μ_1, μ_2 be two probability measures over $B(0, \varepsilon) \subseteq \mathbb{R}^m$ with densities ρ_1, ρ_2 with respect to the uniform probability measure over $B(0, \varepsilon)$ satisfying:*

$$\frac{1}{\alpha} \leq \rho_1(x), \rho_2(x) \leq \alpha,$$

for some $\alpha > 1$. Then

$$W_\infty(\mu_1, \mu_2) \leq \alpha C_m \varepsilon \|\rho_1 - \rho_2\|_{L^\infty(B(0, \varepsilon))},$$

where C_m only depends on dimension m and not on α, ε , or ρ_1, ρ_2 .

Proof. Theorem 1.2. in [23] gives the result for $\varepsilon = 1$. The general case follows immediately from a rescaling argument. \square

Corollary 1. *Let \mathcal{M} be a smooth, compact Riemannian manifold without boundary and let $x \in \mathcal{M}$. Let $\varepsilon < \iota_{\mathcal{M}}/2$. Let μ_1, μ_2 be two probability measures over $B_{\mathcal{M}}(x, \varepsilon)$ with densities ρ_1, ρ_2 , with respect to the uniform probability measure over $B_{\mathcal{M}}(x, \varepsilon)$, that satisfy:*

$$\frac{1}{\alpha} \leq \rho_1(x), \rho_2(x) \leq \alpha,$$

for some $\alpha > 1$. Then

$$W_\infty(\mu_1, \mu_2) \leq \alpha C_{\mathcal{M}} \varepsilon \|\rho_1 - \rho_2\|_{L^\infty(B_{\mathcal{M}}(x, \varepsilon))},$$

where $C_{\mathcal{M}}$ is a manifold dependent constant that does not depend on x, α, ε , or ρ_1, ρ_2 .

Proof. Since for every $x \in \mathcal{M}$ the map $\exp_x : B(0, \varepsilon) \rightarrow B_{\mathcal{M}}(x, \varepsilon)$ is bi-Lipschitz, with bi-Lipschitz constants uniformly bounded over all $0 < \varepsilon < \iota_{\mathcal{M}}/2$ and all $x \in \mathcal{M}$, the desired inequality follows directly from Proposition 3. \square

We also discuss probabilistic bounds for the ∞ -OT distance between μ and the empirical measure μ_n . Specifically, we will use the following result that can be found in [22] (see also references therein).

Theorem 15 (Theorem 2 in [22]). *Let μ_n be the empirical measure of n i.i.d. samples from μ . Then, for any $s > 1$ and $n \in \mathbb{N}$, we have*

$$W_\infty(\mu, \mu_n) = \min_{T: T_\# \mu = \mu_n} \sup_{x \in \mathcal{M}} d_{\mathcal{M}}(T(x), x) \leq A_{\mathcal{M},s} \frac{(\log(n))^{p_m}}{n^{1/m}}, \quad (37)$$

with probability at least $1 - C_{\mathcal{M},s} n^{-s}$, where p_m is a dimension dependent power: $p_m = 3/4$ when $m = 2$, and $p_m = 1/m$ when $m \geq 3$. The constants $C_{\mathcal{M},s}$ and $A_{\mathcal{M},s}$ only depend on s and on \mathcal{M} . In the sequel, we use T_n to denote a minimizer in the above formula.

6.1.3 Proof of Theorem 1

We now provide a proof of Theorem 1, which we restate below for convenience.

Theorem 16 (Ollivier [36]).

$$\left| \kappa_{\mathcal{M}}(x, y) - \frac{\varepsilon^2}{2(m+2)} \text{Ric}_x(v) \right| \leq (C\varepsilon^2 d_{\mathcal{M}}(x, y) + C'\varepsilon^3), \quad (38)$$

where y is a point on the geodesic from x in direction $v \in T_x \mathcal{M}$ and ε is the radius of Ollivier balls.

Proof of Theorem 16. Let $x, y \in \mathcal{M}$ and let $\mathcal{P} : B_{\mathcal{M}}(x, \varepsilon) \rightarrow B_{\mathcal{M}}(y, \varepsilon)$ be the map from (3). Then, according to Proposition 6 in [36], we have

$$d_{\mathcal{M}}(\tilde{x}, \mathcal{P}(\tilde{x})) = d_{\mathcal{M}}(x, y) \left(1 - d_{\mathcal{M}}(x, \tilde{x})^2 \left(\frac{K(v, w)}{2} + O(d_{\mathcal{M}}(x, y) + \varepsilon) \right) \right), \quad (39)$$

where $v = \frac{\log_x(y)}{|\log_x(y)|}$, $w = \log_x(\tilde{x})$, and $K(v, w)$ is the sectional curvature in the plane generated by the vectors $v, w \in T_x \mathcal{M}$. Equation (39) is represented pictorially in Figure 1: the distance between \tilde{x} and $\tilde{y} := \mathcal{P}(\tilde{x})$ is almost equal to the distance between x and y , and the correction term of order 3 is precisely captured by the sectional curvature between vectors v and w .

The measure $\mathcal{P}_\# \mu_x^{\mathcal{M}}$, although not exactly equal to $\mu_y^{\mathcal{M}}$, has a density ρ_{xy} with respect to $\mu_y^{\mathcal{M}}$ that satisfies

$$\sup_{\tilde{y} \in B_{\mathcal{M}}(y, \varepsilon)} |\rho_{xy}(\tilde{y}) - 1| \leq C_{\mathcal{M}}(d_{\mathcal{M}}(x, y)^2 \varepsilon^2 + d_{\mathcal{M}}(x, y) \varepsilon^2),$$

as follows from the discussion in the proof of Proposition 6 in section 8 in [36]. Combining the above estimate with Corollary 1 we get

$$W_\infty(\mathcal{P}_\# \mu_x^{\mathcal{M}}, \mu_y^{\mathcal{M}}) \leq C_{\mathcal{M}} \varepsilon \sup_{\tilde{y} \in B_{\mathcal{M}}(y, \varepsilon)} |\rho_{xy}(\tilde{y}) - 1| \leq C_{\mathcal{M}} d_{\mathcal{M}}(x, y) \varepsilon^3.$$

We can thus find a map $T_y : B_{\mathcal{M}}(y, \varepsilon) \rightarrow B_{\mathcal{M}}(y, \varepsilon)$ such that $T_{y\#}(\mathcal{P}_\# \mu_x^{\mathcal{M}}) = \mu_y^{\mathcal{M}}$ and such that

$$\sup_{y' \in B_{\mathcal{M}}(y, \varepsilon)} |y' - T_y(y')| \leq C'_{\mathcal{M}} d_{\mathcal{M}}(x, y) \varepsilon^3; \quad (40)$$

see [11]. If we now define the function $\mathcal{F} : B_{\mathcal{M}}(x, \varepsilon) \rightarrow B_{\mathcal{M}}(y, \varepsilon)$ as

$$\mathcal{F} := T_y \circ \mathcal{P}, \quad (41)$$

we see that

$$\mathcal{F}_\# \mu_x^{\mathcal{M}} = \mu_y^{\mathcal{M}}.$$

Moreover, for every $\tilde{x} \in B_{\mathcal{M}}(x, \varepsilon)$ we have

$$d_{\mathcal{M}}(\tilde{x}, \mathcal{F}(\tilde{x})) = d_{\mathcal{M}}(x, y) \left(1 - d_{\mathcal{M}}(x, \tilde{x})^2 \left(\frac{K(v, w)}{2} + O(d_{\mathcal{M}}(x, y) + \varepsilon) \right) \right), \quad (42)$$

where we recall $v = \frac{\log_x(y)}{|\log_x(y)|}$ and $w = \log_x(\tilde{x})$. It follows that

$$\begin{aligned} W_1(\mu_x^{\mathcal{M}}, \mu_y^{\mathcal{M}}) &\leq \int_{B_{\mathcal{M}}(x, \varepsilon)} d_{\mathcal{M}}(\tilde{x}, \mathcal{F}(\tilde{x})) d\mu_x^{\mathcal{M}}(\tilde{x}) \\ &\leq d_{\mathcal{M}}(x, y) - \varepsilon^2 d_{\mathcal{M}}(x, y) \frac{\text{Ric}_x(v)}{2(m+2)} + O(d_{\mathcal{M}}(x, y)^2 \varepsilon^2 + d_{\mathcal{M}}(x, y) \varepsilon^3), \end{aligned} \quad (43)$$

and in turn

$$\frac{1}{\varepsilon^2} \kappa_{\mathcal{M}}(x, y) + O(d_{\mathcal{M}}(x, y) + \varepsilon) \geq \frac{\text{Ric}_x(v)}{2(m+2)},$$

giving a lower bound for $\kappa_{\mathcal{M}}$.

To obtain a matching upper bound, we follow [36] and construct a function $f : \mathcal{M} \rightarrow \mathbb{R}$ that is 1-Lipschitz with respect to $d_{\mathcal{M}}(\cdot, \cdot)$ and that almost realizes the sup in the Kantorovich-Rubinstein dual formulation of the 1-Wasserstein distance between $\mu_x^{\mathcal{M}}$ and $\mu_y^{\mathcal{M}}$ (see Theorem 14). To define this function, let us consider $0 < r_0 < \iota_{\mathcal{M}}$, and suppose that ε is small enough and x, y are sufficiently close so that $B_{\mathcal{M}}(x, \varepsilon), B_{\mathcal{M}}(y, \varepsilon) \subseteq B_{\mathcal{M}}(x, r_0/4)$. Let $E_0 := \{v' \in T_x \mathcal{M} : \langle v', \log_x(y) \rangle = 0\}$. We first define $f : B_{\mathcal{M}}(x, r_0) \rightarrow \mathbb{R}$ by

$$f(z) := \begin{cases} \text{dist}(z, \exp_x(E_0)) & \text{if } \langle \log_x(z), \log_x(y) \rangle \geq 0 \\ -\text{dist}(z, \exp_x(E_0)) & \text{if } \langle \log_x(z), \log_x(y) \rangle < 0, \end{cases} \quad (44)$$

which is 1-Lipschitz in its domain, and then extend it to a global 1-Lipschitz function using the McShane-Whitney extension theorem. Following the steps in section 8 in [36] we can then see that

$$f(\mathcal{F}(\tilde{x})) - f(\tilde{x}) = d_{\mathcal{M}}(x, y) \left(1 - d_{\mathcal{M}}(x, \tilde{x})^2 \left(\frac{K(v, w)}{2} + O(d_{\mathcal{M}}(x, y) + \varepsilon) \right) \right) \quad (45)$$

for every $\tilde{x} \in B_{\mathcal{M}}(x, \varepsilon)$, where we recall $v = \frac{\log_x(y)}{|\log_x(y)|}, w = \log_x(\tilde{x})$ and \mathcal{F} is as in (41). Integrating with respect to $\mu_x^{\mathcal{M}}$ and using the Kantorovich-Rubinstein

theorem we get

$$\begin{aligned}
W_1(\mu_x^{\mathcal{M}}, \mu_y^{\mathcal{M}}) &\geq \int_{\mathcal{M}} f(\tilde{y}) d\mu_y^{\mathcal{M}}(\tilde{y}) - \int_{\mathcal{M}} f(\tilde{x}) d\mu_x^{\mathcal{M}}(\tilde{x}) \\
&= \int_{\mathcal{M}} f(\mathcal{F}(\tilde{x})) d\mu_x^{\mathcal{M}}(\tilde{x}) - \int_{\mathcal{M}} f(\tilde{x}) d\mu_x^{\mathcal{M}}(\tilde{x}) \\
&= d_{\mathcal{M}}(x, y) - \varepsilon^2 d_{\mathcal{M}}(x, y) \frac{\text{Ric}_x(v)}{2(m+2)} + O(d_{\mathcal{M}}(x, y)^2 \varepsilon^2 + d_{\mathcal{M}}(x, y) \varepsilon^3),
\end{aligned} \tag{46}$$

from where we can now obtain

$$\frac{1}{\varepsilon^2} \kappa_{\mathcal{M}}(x, y) \leq \frac{\text{Ric}_x(v)}{2(m+2)} + O(d_{\mathcal{M}}(x, y) + \varepsilon).$$

□

6.1.4 Some additional lemmas

In this section we collect a few lemmas that we use in the proof of our main results.

Lemma 4. *There is a constant c such that for all small enough $\varepsilon_0 > 0$ and all $x \in \mathcal{M}$ we have*

$$v_m(1 - c\varepsilon_0^2)\varepsilon_0^m \leq \text{vol}(B_{\mathcal{M}}(x, \varepsilon_0)) \leq v_m(1 + c\varepsilon_0^2)\varepsilon_0^m,$$

where v_m is the volume of the m -dimensional Euclidean ball.

Moreover, if $\varepsilon_0 > 0$ is such that $W_{\infty}(\mu, \mu_n) \leq \frac{1}{2}\varepsilon_0$, then

$$\mu(B_{\mathcal{M}}(x, \varepsilon_0 - W_{\infty}(\mu, \mu_n))) \leq \mu_n(B_{\mathcal{M}}(x, \varepsilon_0)) \leq \mu(B_{\mathcal{M}}(x, \varepsilon_0 + W_{\infty}(\mu, \mu_n))).$$

Proof. The first part is a standard result in differential geometry (see for example 1.35 in [22]). The second part is immediate from the definition of $W_{\infty}(\mu, \mu_n)$. □

Given the assumed compactness and smoothness of the manifold \mathcal{M} , it is straightforward to show that there exists a constant $C_{\mathcal{M}} \geq 1$ such that

$$\mu_x^{\mathcal{M}}(B_{\mathcal{M}}(x, \varepsilon) \setminus (B_{\mathcal{M}}(x, \varepsilon) \cap B_{\mathcal{M}}(y, \varepsilon))) \leq C_{\mathcal{M}} \frac{d_{\mathcal{M}}(x, y)}{\varepsilon} \tag{47}$$

for all $x, y \in \mathcal{M}$ and all $\varepsilon \leq \iota_{\mathcal{M}}/2$; indeed, this type of estimate is easily proved in Euclidean space and can be extended to the manifold setting for all small enough ε using coarse bounds on the metric distortion by the exponential map around a given point on the manifold. With the aid of standard concentration inequalities we can get a similar estimate to (47) when $x \in \mathcal{X}$ and $\mu_x^{\mathcal{M}}$ is replaced with the empirical measure μ_x^G . This is the content of the next lemma.

Lemma 5. *Provided that $\frac{W_\infty(\mu, \mu_n)}{\varepsilon}$ is sufficiently small, we have*

$$\frac{\mu_n(B_{\mathcal{M}}(x, \varepsilon) \setminus B_{\mathcal{M}}(x, \varepsilon) \cap B_{\mathcal{M}}(y, \varepsilon))}{\mu_n(B_{\mathcal{M}}(x, \varepsilon))} \leq \frac{\psi(0)c_0}{6}$$

for all $x, y \in \mathcal{X}$ satisfying $0 < d_{\mathcal{M}}(x, y) \leq \frac{\psi(0)}{12C_{\mathcal{M}}}\delta_0$.

Proof. This result follows from (47), Lemma 4, and the smallness assumption of $W_\infty(\mu, \mu_n)$ relative to ε . \square

6.2 Proofs of global curvature bounds

We start by proving Theorem 10.

Proof of Theorem 10. Thanks to Lemma 2 it is enough to prove the lower bound under the assumption that $x, y \in \mathcal{X}$ are two distinct points such that $d_{G, \mathcal{M}}(x, y) = \tilde{d}_{G, \mathcal{M}}(x, y) \leq \delta_1$. Notice that $\tilde{d}_{G, \mathcal{M}}(x, y) = \delta_0 \psi(d_{\mathcal{M}}(x, y)/\delta_0)$ and thus we may further split the analysis into different cases determined by the value of $d_{\mathcal{M}}(x, y)$. It is worth recalling that in the setting considered here we have $B_G(x, \varepsilon) = B_{\mathcal{M}}(x, \varepsilon) \cap \mathcal{X}$ and $B_G(y, \varepsilon) = B_{\mathcal{M}}(y, \varepsilon) \cap \mathcal{X}$.

Case 1: $0 < d_{\mathcal{M}}(x, y) \leq \frac{\psi(0)}{12C_{\mathcal{M}}}\delta_0$, where $C_{\mathcal{M}}$ is as in (47).

We may assume without the loss of generality that $|B_G(x, \varepsilon)| \geq |B_G(y, \varepsilon)|$, for otherwise we can swap the roles of x and y . From Lemma 5 it follows

$$\mu_x^G(B_{\mathcal{M}}(x, \varepsilon) \setminus (B_{\mathcal{M}}(x, \varepsilon) \cap B_{\mathcal{M}}(y, \varepsilon))) \leq \frac{\psi(0)c_0}{6}.$$

Also, for all $\tilde{x} \in B_G(x, \varepsilon)$ and $\tilde{y} \in B_G(y, \varepsilon)$ we have

$$d_{G, \mathcal{M}}(\tilde{x}, \tilde{y}) \leq d_{G, \mathcal{M}}(x, \tilde{x}) + d_{G, \mathcal{M}}(\tilde{x}, \tilde{y}) + d_{G, \mathcal{M}}(\tilde{y}, y) \leq 2\delta_0 \psi(\varepsilon/\delta_0) + \delta_0 \leq 3\varepsilon.$$

By selecting a coupling between μ_x^G and μ_y^G that leaves all mass of μ_x^G in $B_{\mathcal{M}}(x, \varepsilon) \cap B_{\mathcal{M}}(y, \varepsilon)$ fixed, the above estimates imply

$$W_{1, G}(\mu_x^G, \mu_y^G) \leq 3\varepsilon \mu_x^G(B_{\mathcal{M}}(x, \varepsilon) \setminus (B_{\mathcal{M}}(x, \varepsilon) \cap B_{\mathcal{M}}(y, \varepsilon))) \leq \frac{1}{2} \psi(0) \delta_0.$$

In addition, since by definition we have $d_{G, \mathcal{M}}(x, y) = \tilde{d}_{G, \mathcal{M}}(x, y) \geq \delta_0 \psi(0)$, it follows

$$\frac{\kappa_G(x, y)}{\varepsilon^2} = \frac{1}{\varepsilon^2} \left(1 - \frac{W_{1, G}(\mu_x^G, \mu_y^G)}{d_{G, \mathcal{M}}(x, y)} \right) \geq \frac{1}{2\varepsilon^2}.$$

Case 2: $\frac{\psi(0)}{12C_{\mathcal{M}}}\delta_0 \leq d_{\mathcal{M}}(x, y) \leq \delta_1 - 2\varepsilon$.

We start by finding a good upper bound for $W_{1, G}(\mu_x^G, \mu_y^G)$. Without the loss of generality we can assume that

$$a := \frac{\mu(B_{\mathcal{M}}(x, \varepsilon))}{\mu_n(B_G(x, \varepsilon))} \leq \frac{\mu(B_{\mathcal{M}}(y, \varepsilon))}{\mu_n(B_G(y, \varepsilon))},$$

for otherwise we can swap the roles of x and y . We split the measure μ_x^G into

$$\mu_x^G = \mu_x^G \lfloor_{B_{\mathcal{M}}(x, \varepsilon')} + \mu_x^G \lfloor_{B_{\mathcal{M}}(x, \varepsilon) \setminus B_{\mathcal{M}}(x, \varepsilon')},$$

where $\varepsilon' := \varepsilon - 3W_\infty(\mu, \mu_n) - C'_{\mathcal{M}}\varepsilon^4$ and where the measures on the right hand side represent the restrictions of μ_x^G to $B_{\mathcal{M}}(x, \varepsilon')$ and $B_{\mathcal{M}}(x, \varepsilon) \setminus B_{\mathcal{M}}(x, \varepsilon')$, respectively. We decompose the measure μ_y^G as

$$\mu_y^G = \mu_{y,1}^G + \mu_{y,2}^G$$

for two positive measures $\mu_{y,1}^G$ and $\mu_{y,2}^G$ that we define below, the first of which will be suitably coupled with $\mu_x^G \lfloor_{B_{\mathcal{M}}(x, \varepsilon')}$ while the second one will be coupled with $\mu_x^G \lfloor_{B_{\mathcal{M}}(x, \varepsilon) \setminus B_{\mathcal{M}}(x, \varepsilon')}$.

Precisely, the measure $\mu_{y,1}^G$ is defined as

$$\mu_{y,1}^G := aT_{n\sharp}(\mathcal{F}_\sharp(\mu_x^{\mathcal{M}} \lfloor_{T_n^{-1}(B_{\mathcal{M}}(x, \varepsilon'))})),$$

where $T_n : \mathcal{M} \rightarrow \mathcal{X}$ is an ∞ -OT map between μ and μ_n as defined in Theorem 15 and \mathcal{F} is the map defined in (41). We will show that $\mu_{y,1}^G \leq \mu_y^G$, which would allow us to take $\mu_{y,2}^G := \mu_y^G - \mu_{y,1}^G$. To see that indeed $\mu_{y,1}^G \leq \mu_y^G$, we first observe that $T_n^{-1}(B_{\mathcal{M}}(x, \varepsilon'))$ is contained in $B_{\mathcal{M}}(x, \varepsilon - 2W_\infty(\mu, \mu_n) - C'_{\mathcal{M}}\varepsilon^4)$. From (40) and ii) in Assumption 3 it follows that $\mathcal{F}(T_n^{-1}(B_{\mathcal{M}}(x, \varepsilon'))) \subseteq B_{\mathcal{M}}(y, \varepsilon - 2W_\infty(\mu, \mu_n))$. Finally, $T_n(\mathcal{F}(T_n^{-1}(B_{\mathcal{M}}(x, \varepsilon')))) \subseteq B_{\mathcal{M}}(y, \varepsilon - W_\infty(\mu, \mu_n))$. From this we see that the support of $\mu_{y,1}^G$ is contained in $B_{\mathcal{M}}(y, \varepsilon - W_\infty(\mu, \mu_n))$. Now, let $A \subseteq B_{\mathcal{M}}(y, \varepsilon - W_\infty(\mu, \mu_n))$. We see that

$$\begin{aligned} \mu_{y,1}^G(A) &= a\mu_x^{\mathcal{M}}(T_n^{-1}(B_{\mathcal{M}}(x, \varepsilon')) \cap \mathcal{F}^{-1}(T_n^{-1}(A))) \\ &\leq a\mu_x^{\mathcal{M}}(\mathcal{F}^{-1}(T_n^{-1}(A))) \\ &= a\mu_y^{\mathcal{M}}(T_n^{-1}(A)) \\ &= \frac{a}{\mu(B_{\mathcal{M}}(y, \varepsilon))} \mu(T_n^{-1}(A)) \\ &= \frac{a}{\mu(B_{\mathcal{M}}(y, \varepsilon))} \mu_n(A) \\ &= \frac{a\mu_n(B_G(y, \varepsilon))}{\mu(B_{\mathcal{M}}(y, \varepsilon))} \mu_y^G(A) \\ &\leq \mu_y^G(A). \end{aligned}$$

In the above, the second equality follows from the fact that $T_n^{-1}(A) \subseteq B_{\mathcal{M}}(y, \varepsilon)$ and the fact that $\mathcal{F}_\sharp \mu_x^{\mathcal{M}} = \mu_y^{\mathcal{M}}$; the fourth equality follows from the fact that $T_{n\sharp} \mu = \mu_n$; the last inequality follows from the definition of a . Since A was arbitrary, we conclude that indeed $\mu_{y,1}^G \leq \mu_y^G$.

Next, we show that $\mu_x^G \lfloor_{B_{\mathcal{M}}(x, \varepsilon')}$ and $\mu_{y,1}^G$ have the same total mass and then construct a suitable coupling between them. Indeed, on one hand we have

$\mu_x^G \lfloor_{B_{\mathcal{M}}(x, \varepsilon')}(\mathcal{X}) = \mu_x^G(B_{\mathcal{M}}(x, \varepsilon')) = \frac{\mu_n(B_{\mathcal{M}}(x, \varepsilon'))}{\mu_n(B_G(x, \varepsilon))}$. On the other hand,

$$\begin{aligned}\mu_{y,1}^G(\mathcal{X}) &= a\mu_x^{\mathcal{M}}(T_n^{-1}(B_{\mathcal{M}}(x, \varepsilon'))) = \frac{a}{\mu(B_{\mathcal{M}}(x, \varepsilon))}\mu(T_n^{-1}(B_{\mathcal{M}}(x, \varepsilon'))) \\ &= \frac{a}{\mu(B_{\mathcal{M}}(x, \varepsilon))}\mu_n(B_{\mathcal{M}}(x, \varepsilon')) = \frac{\mu_n(B_{\mathcal{M}}(x, \varepsilon'))}{\mu_n(B_G(x, \varepsilon))},\end{aligned}$$

which implies that the measures indeed have the same total mass. To construct a suitable coupling $\pi_1^G \in \Gamma(\mu_x^G \lfloor_{B_{\mathcal{M}}(x, \varepsilon')}, \mu_{y,1}^G)$, we first introduce the measure

$$\tilde{\nu}_1 := \frac{a}{\mu(B_{\mathcal{M}}(x, \varepsilon))}\mu \lfloor_{T_n^{-1}(B_{\mathcal{M}}(x, \varepsilon'))}.$$

Observe that $\tilde{\pi}_1 := (T_n \times Id)_{\#}\tilde{\nu}_1$ belongs to $\Gamma(\mu_x^G \lfloor_{B_{\mathcal{M}}(x, \varepsilon')}, \tilde{\nu}_1)$ and

$$d_{\mathcal{M}}(\tilde{x}, \tilde{x}') \leq W_{\infty}(\mu, \mu_n), \quad \forall (\tilde{x}, \tilde{x}') \in \text{spt}(\tilde{\pi}_1).$$

Also, $\tilde{\pi}_2 := (Id \times \mathcal{F})_{\#}\tilde{\nu}_1 \in \Gamma(\tilde{\nu}_1, \mathcal{F}_{\#}\tilde{\nu}_1)$ satisfies

$$d_{\mathcal{M}}(\tilde{x}', \tilde{y}') = d_{\mathcal{M}}(x, y) \left(1 - d_{\mathcal{M}}(x, \tilde{x}')^2 \left(\frac{K(v, w')}{2} + O(d_{\mathcal{M}}(x, y) + \varepsilon) \right) \right)$$

for all $(\tilde{x}', \tilde{y}') \in \text{spt}(\tilde{\pi}_2)$, according to (42); in the above, $v = \frac{\log_x(y)}{|\log_x(y)|}$ and $w' = \log_x(\tilde{x}')$. Finally, $\tilde{\pi}_3 := (Id \times T_n)_{\#}(\mathcal{F}_{\#}\tilde{\nu}_1) \in \Gamma(\mathcal{F}_{\#}\tilde{\nu}_1, \mu_{y,1}^G)$ satisfies

$$d_{\mathcal{M}}(\tilde{y}', \tilde{y}) \leq W_{\infty}(\mu, \mu_n), \quad \forall (\tilde{y}', \tilde{y}) \in \text{spt}(\tilde{\pi}_3).$$

We can then define $\pi_1^G \in \Gamma(\mu_x^G \lfloor_{B_{\mathcal{M}}(x, \varepsilon')}, \mu_{y,1}^G)$ as

$$\pi_1^G := T_{1,4\#}\Pi.$$

where Π is the glueing of the couplings $\tilde{\pi}_1, \tilde{\pi}_2, \tilde{\pi}_3$ as defined in (35) and $T_{1,4}$ is the projection onto the first and fourth coordinates introduced when we defined the glueing of couplings.

We now proceed to estimate $W_{1,G}(\mu_x^G, \mu_y^G)$ from above using the coupling π_1^G . First, let $(\tilde{x}, \tilde{x}', \tilde{y}', \tilde{y}) \in \text{spt}(\Pi)$. From the above discussion we have

$$d_{\mathcal{M}}(\tilde{x}, \tilde{y}) = d_{\mathcal{M}}(x, y) \left(1 - d_{\mathcal{M}}(x, \tilde{x}')^2 \left(\frac{K(v, w')}{2} + O(d_{\mathcal{M}}(x, y) + \varepsilon) \right) \right) + O(W_{\infty}(\mu, \mu_n)).$$

In particular, given the smallness of $W_{\infty}(\mu, \mu_n)$ relative to ε and the fact that $d_{\mathcal{M}}(x, y) \leq \delta_1 - 2\varepsilon$ we can assume without the loss of generality that $d_{\mathcal{M}}(\tilde{x}, \tilde{y}) \leq \delta_1$ and thus

$$d_{G,\mathcal{M}}(\tilde{x}, \tilde{y}) \leq \tilde{d}_{G,\mathcal{M}}(\tilde{x}, \tilde{y}) = \delta_0\psi(d_{\mathcal{M}}(\tilde{x}, \tilde{y})/\delta_0).$$

Using the fact that ψ is non-decreasing combined with a simple Taylor expansion of ψ around $d_{\mathcal{M}}(x, y)/\delta_0$, we can bound the right hand side of the above by

$$\begin{aligned} & \delta_0 \psi \left(\frac{d_{\mathcal{M}}(x, y)}{\delta_0} \right) + \psi' \left(\frac{d_{\mathcal{M}}(x, y)}{\delta_0} \right) (d_{\mathcal{M}}(\tilde{x}, \tilde{y}) - d_{\mathcal{M}}(x, y)) \\ & \quad + \frac{1}{2\delta_0} \|\psi''\|_{\infty} (d_{\mathcal{M}}(\tilde{x}, \tilde{y}) - d_{\mathcal{M}}(x, y))^2 \\ & \leq \delta_0 \psi \left(\frac{d_{\mathcal{M}}(x, y)}{\delta_0} \right) - \frac{1}{2} \psi' \left(\frac{d_{\mathcal{M}}(x, y)}{\delta_0} \right) d_{\mathcal{M}}(x, y) \varepsilon^2 K(v, w') \\ & \quad + O(\varepsilon^4 + W_{\infty}(\mu, \mu_n)); \end{aligned}$$

notice that $\|\psi''\|_{\infty}$, the supremum norm of the second derivative of ψ , is finite by Assumption 2; notice also that this second order correction term is of order $O(W_{\infty}(\mu, \mu_n)^2/\varepsilon + \varepsilon^5)$, which is much smaller than $O(\varepsilon^4 + W_{\infty}(\mu, \mu_n))$.

From the above estimates we get

$$\begin{aligned} W_{1,G}(\mu_x^G \lfloor_{B_{\mathcal{M}}(x,\varepsilon')}, \mu_{y,1}^G) & \leq \int d_{G,\mathcal{M}}(\tilde{x}, \tilde{y}) d\pi_1^G(\tilde{x}, \tilde{y}) = \int d_{G,\mathcal{M}}(\tilde{x}, \tilde{y}) d\Pi(\tilde{x}, \tilde{x}', \tilde{y}', \tilde{y}) \\ & \leq \delta_0 \psi(d_{\mathcal{M}}(x, y)/\delta_0) - \frac{1}{2} \psi' \left(\frac{d_{\mathcal{M}}(x, y)}{\delta_0} \right) d_{\mathcal{M}}(x, y) \int d_{\mathcal{M}}(x, \tilde{x}')^2 K(v, \log_x(\tilde{x}')) d\tilde{\nu}_1(\tilde{x}') \\ & \quad + C(\varepsilon^4 + W_{\infty}(\mu, \mu_n)) \\ & \leq \delta_0 \psi(d_{\mathcal{M}}(x, y)/\delta_0) - \frac{1}{2} \psi' \left(\frac{d_{\mathcal{M}}(x, y)}{\delta_0} \right) d_{\mathcal{M}}(x, y) \int d_{\mathcal{M}}(x, \tilde{x}')^2 K(v, \log_x(\tilde{x}')) d\mu_x^{\mathcal{M}}(\tilde{x}') \\ & \quad + C(\varepsilon^4 + W_{\infty}(\mu, \mu_n)) \\ & \leq \delta_0 \psi(d_{\mathcal{M}}(x, y)/\delta_0) - \psi' \left(\frac{d_{\mathcal{M}}(x, y)}{\delta_0} \right) d_{\mathcal{M}}(x, y) \varepsilon^2 \frac{\text{Ric}_x(v)}{2(m+2)} \\ & \quad + C(\varepsilon^4 + W_{\infty}(\mu, \mu_n)). \end{aligned} \tag{48}$$

In the second to last inequality we have substituted the integral with respect to $\tilde{\nu}_1$ with an integral with respect to $\mu_x^{\mathcal{M}}$ by introducing an error that is of much smaller order than $W_{\infty}(\mu, \mu_n) + \varepsilon^4$, thanks to Lemma 4; in the last inequality we have used (42) and (43).

Next, we find a bound for $W_{1,G}(\mu_x^G \lfloor_{B_{\mathcal{M}}(x,\varepsilon) \setminus B_{\mathcal{M}}(x,\varepsilon')}, \mu_{y,2}^G)$. We observe that for every $\tilde{x} \in B_G(x, \varepsilon)$ we have $d_{G,\mathcal{M}}(\tilde{x}, x) \leq \max\{\delta_0, d_{\mathcal{M}}(\tilde{x}, x)\} \leq \varepsilon$. Likewise, for every $\tilde{y} \in B_G(y, \varepsilon)$ we have $d_{G,\mathcal{M}}(\tilde{y}, y) \leq \max\{\delta_0, d_{\mathcal{M}}(\tilde{y}, y)\} \leq \varepsilon$. Additionally, $d_{G,\mathcal{M}}(x, y) \leq d_{\mathcal{M}}(x, y) \leq \delta_1 = c_1 \varepsilon$. It follows that $d_{G,\mathcal{M}}(\tilde{x}, \tilde{y}) \leq C\varepsilon$ for all $\tilde{x} \in B_G(x, \varepsilon)$ and $\tilde{y} \in B_G(y, \varepsilon)$. This implies

$$\begin{aligned} W_{1,G}(\mu_x^G \lfloor_{B_{\mathcal{M}}(x,\varepsilon) \setminus B_{\mathcal{M}}(x,\varepsilon')}, \mu_{y,2}^G) & \leq C\varepsilon \frac{\mu_n(B_{\mathcal{M}}(x, \varepsilon) \setminus B_{\mathcal{M}}(x, \varepsilon'))}{\mu_n(B_{\mathcal{M}}(x, \varepsilon))} \\ & \leq C(W_{\infty}(\mu, \mu_n) + \varepsilon^4), \end{aligned}$$

thanks to Lemma 4.

We may now invoke Lemma 3 and (48) to get

$$\begin{aligned}
W_{1,G}(\mu_x^G, \mu_y^G) &\leq W_{1,G}(\mu_x^G \lfloor_{B_{\mathcal{M}}(x,\varepsilon')}, \mu_{y,1}^G) + W_{1,G}(\mu_x^G \lfloor_{B_{\mathcal{M}}(x,\varepsilon) \setminus B_{\mathcal{M}}(x,\varepsilon')}, \mu_{y,2}^G) \\
&\leq \delta_0 \psi(d_{\mathcal{M}}(x,y)/\delta_0) - \psi' \left(\frac{d_{\mathcal{M}}(x,y)}{\delta_0} \right) d_{\mathcal{M}}(x,y) \varepsilon^2 \frac{\text{Ric}_x(v)}{2(m+2)} \\
&\quad + C(\varepsilon^4 + W_\infty(\mu, \mu_n)).
\end{aligned} \tag{49}$$

Recalling that $d_{G,\mathcal{M}}(x,y) = \delta_0 \psi(d_{\mathcal{M}}(x,y)/\delta_0) \geq \delta_0 \psi(0) = c_0 \psi(0) \varepsilon$, we deduce

$$\begin{aligned}
\frac{\kappa_G(x,y)}{\varepsilon^2} &= \frac{1}{\varepsilon^2} \left(1 - \frac{W_{1,G}(\mu_x^G, \mu_y^G)}{d_{G,\mathcal{M}}(x,y)} \right) \geq \psi' \left(\frac{d_{\mathcal{M}}(x,y)}{\delta_0} \right) \frac{d_{\mathcal{M}}(x,y)}{\delta_0 \psi \left(\frac{d_{\mathcal{M}}(x,y)}{\delta_0} \right)} \frac{\text{Ric}_x(v)}{2(m+2)} \\
&\quad - C \left(\varepsilon + \frac{W_\infty(\mu, \mu_n)}{\varepsilon^3} \right).
\end{aligned} \tag{50}$$

Under the assumption that $\text{Ric}_x(v) \geq 2(D+2)K \geq 0$, the first term on the right hand side can be bounded from below by $\psi'(0) \frac{c_0 \psi(0)}{12c_1 C_{\mathcal{M}}} K$. If, on the other hand, $K < 0$, then the first term on the right hand side of (50) can be bounded from below by $\frac{c_1}{c_0 \psi(0)} K$.

Case 3: Here we assume that $\delta_1 \geq d_{\mathcal{M}}(x,y) \geq \delta_1 - 2\varepsilon$.

According to Assumption 3 we have $d_{\mathcal{M}}(x,y) \geq 2\delta_0$ and in particular $d_{G,\mathcal{M}}(x,y) = \delta_0 \psi \left(\frac{d_{\mathcal{M}}(x,y)}{\delta_0} \right) = d_{\mathcal{M}}(x,y)$. Let \bar{x} be the midpoint between x and y along a (manifold) minimizing geodesic connecting them; \bar{x} may not be a point in \mathcal{X} , but this is unimportant for our argument. Now, notice that $d_{\mathcal{M}}(x,\bar{x}) = \frac{1}{2} d_{\mathcal{M}}(x,y) \in [2\delta_0, \delta_1 - 2\varepsilon]$ and also $d_{\mathcal{M}}(\bar{x},y) = \frac{1}{2} d_{\mathcal{M}}(x,y) \in [2\delta_0, \delta_1 - 2\varepsilon]$. Using the triangle inequality for $W_{1,G}$ and recalling Remark 2 we get:

$$W_{1,G}(\mu_x^G, \mu_y^G) \leq W_{1,G}(\mu_x^G, \mu_{\bar{x}}^G) + W_{1,G}(\mu_{\bar{x}}^G, \mu_y^G).$$

Then

$$\begin{aligned}
\kappa_G(x,y) &= 1 - \frac{W_{1,G}(\mu_x^G, \mu_y^G)}{d_{G,\mathcal{M}}(x,y)} \\
&\geq 1 - \frac{W_{1,G}(\mu_x^G, \mu_y^G)}{d_{\mathcal{M}}(x,y)} \\
&\geq 1 - \frac{W_{1,G}(\mu_x^G, \mu_{\bar{x}}^G) + W_{1,G}(\mu_{\bar{x}}^G, \mu_y^G)}{d_{\mathcal{M}}(x,y)} \\
&= \frac{1}{2} \left(1 - \frac{W_{1,G}(\mu_x^G, \mu_{\bar{x}}^G)}{d_{\mathcal{M}}(x,\bar{x})} \right) + \frac{1}{2} \left(1 - \frac{W_{1,G}(\mu_{\bar{x}}^G, \mu_y^G)}{d_{\mathcal{M}}(\bar{x},y)} \right).
\end{aligned}$$

Using (49) twice (which can be applied regardless of whether $\bar{x} \in \mathcal{X}$ or not), and noticing that $\psi(d_{\mathcal{M}}(x,y)/2\delta_0) = d_{\mathcal{M}}(x,y)/2\delta_0$ and $\psi'(d_{\mathcal{M}}(x,y)/2\delta_0) = 1$, we

can lower bound each of the terms on the right hand side of the above expression by $\frac{1}{2}(s_K \varepsilon^2 K - C \left(\varepsilon^3 + \frac{W_\infty(\mu, \mu_n)}{\varepsilon} \right))$. □

Remark 17. *We would like to highlight the different ways in which $W_{1,G}(\mu_x^G, \mu_y^G)$ is bounded in Cases 1 and 2 in the previous proof. Indeed, in Case 1, when $d_{\mathcal{M}}(x, y)$ is very small, we choose a coupling between μ_x^G and μ_y^G that leaves most mass fixed, taking advantage of the fact that the overlap between $B_G(x, \varepsilon)$ and $B_G(y, \varepsilon)$ is large in this case. In Case 2, on the other hand, the coupling that we use mimics the coupling in the proof of Theorem 1, where all mass moves parallel to the geodesic connecting x and y . Notice that we do need to split into these two cases: in going from (49) to the final lower bound in Case 2 we need to have a lower bound on $d_{\mathcal{M}}(x, y)$ that is $O(\varepsilon)$ (for the case $K > 0$).*

Notice also that the profile function ψ can not be taken to be the identity map for all $t > 0$. Indeed, when we divide $W_{1,G}(\mu_x^G, \mu_y^G)$ by $\delta_0 \psi(0)$ to go from (49) to (50), we need $\psi(0) > 0$ to guarantee that the term $\frac{1}{\delta_0 \psi(0) \varepsilon^2} (\varepsilon^4 + W_\infty(\mu, \mu_n))$ is indeed small regardless of how small $d_{\mathcal{M}}(x, y)$ may be. Since the minimum interpoint distance in a data set is much smaller than $O(1/n^{1/m})$, the distance $d_{\mathcal{M}}(x, y)$ may indeed be quite small. This forces us to consider a profile function ψ that bends away, smoothly (so that the first order Taylor expansion of ψ can reveal the desired curvature term), from the diagonal. The factor s_K in the lower bound (10) arises when lower bounding κ_G for x, y for which $O(\delta) \leq d_{\mathcal{M}}(x, y) \leq \delta_0$. We can think of this range as the transition from the Riemannian lengthscale, where \mathcal{M} 's geometry can be captured, to a lengthscale where the RGG exhibits complete graph behavior. A somewhat similar separation of scales in an RGG was used in [21] to study the convergence of discrete Wasserstein spaces defined over RGGs toward the standard Wasserstein space; see the discussions in Remark 1.16. and section 2.1 in [21].

We now proceed to prove Theorem 13. The proof is very similar to the one for Theorem 10 and thus we will mostly provide details for the steps that need some adjustments. In particular, we highlight the reason for requiring \hat{d}_g to approximate $d_{\mathcal{M}}$ up to an error of order four; see Remark 18 below.

Proof of Theorem 13. Thanks to Lemma 1 we can assume, without the loss of generality, that $x, y \in \mathcal{X}$ are such that $d_{G, \mathcal{X}}(x, y) = \tilde{d}_{G, \mathcal{X}}(x, y) = \delta_0 \psi \left(\frac{\hat{d}_g(x, y)}{\delta_0} \right) \leq \delta_1$. As in Theorem 10 we split our analysis into three different cases. We recall that Ollivier balls in this setting take the form:

$$B_G(x, \varepsilon) = \{\tilde{x} \in \mathcal{X} : \hat{d}_g(x, \tilde{x}) \leq \varepsilon\}, \quad B_G(y, \varepsilon) = \{\tilde{y} \in \mathcal{X} : \hat{d}_g(y, \tilde{y}) \leq \varepsilon\}. \quad (51)$$

Case 1: $0 < \hat{d}_g(x, y) \leq \frac{\psi(0)}{12C_{\mathcal{M}}} \delta_0$, where $C_{\mathcal{M}}$ is as in (47).

We may assume without the loss of generality that $|B_G(x, \varepsilon)| \geq |B_G(y, \varepsilon)|$, for otherwise we can swap the roles of x and y . For $\varepsilon_{\pm} := \varepsilon \pm (C_1 \beta \varepsilon^3 + C_2 \varepsilon^4)$,

thanks to (16) and Lemmas 4 and 5 we can assume

$$\mu_x^G(B_G(x, \varepsilon) \setminus (B_G(x, \varepsilon) \cap B_G(y, \varepsilon))) \leq \frac{36\psi(0)c_0}{12^2}.$$

Now, for all $\tilde{x} \in B_G(x, \varepsilon)$ and $\tilde{y} \in B_G(y, \varepsilon)$ we have

$$d_{G, \mathcal{X}}(\tilde{x}, \tilde{y}) \leq d_{G, \mathcal{X}}(x, \tilde{x}) + d_{G, \mathcal{X}}(\tilde{x}, \tilde{y}) + d_{G, \mathcal{X}}(\tilde{y}, y) \leq 2\delta_0\psi(\varepsilon/\delta_0) + \delta_0 \leq 3\varepsilon.$$

By selecting a coupling between μ_x^G and μ_y^G that leaves all mass of μ_x^G in $B_G(x, \varepsilon) \cap B_G(y, \varepsilon)$ fixed, the above estimates imply

$$W_{1,G}(\mu_x^G, \mu_y^G) \leq 3\varepsilon\mu_x^G(B_G(x, \varepsilon) \setminus (B_G(x, \varepsilon) \cap B_G(y, \varepsilon))) \leq \frac{3}{4}\psi(0)\delta_0.$$

In addition, since by definition we have $d_{G, \mathcal{X}}(x, y) = \tilde{d}_{G, \mathcal{X}}(x, y) \geq \delta_0\psi(0)$, it follows

$$\frac{\kappa_G(x, y)}{\varepsilon^2} = \frac{1}{\varepsilon^2} \left(1 - \frac{W_{1,G}(\mu_x^G, \mu_y^G)}{d_{G, \mathcal{X}}(x, y)} \right) \geq \frac{1}{4\varepsilon^2}.$$

Case 2: $\frac{\psi(0)}{12C_{\mathcal{M}}}\delta_0 \leq \hat{d}_g(x, y) \leq \delta_1 - 2\varepsilon$.

As in the proof of Theorem 10 we may further assume, without the loss of generality, that

$$a := \frac{\mu(B_{\mathcal{M}}(x, \varepsilon))}{\mu_n(B_G(x, \varepsilon))} \leq \frac{\mu(B_{\mathcal{M}}(y, \varepsilon))}{\mu_n(B_G(y, \varepsilon))}.$$

The measure μ_x^G is decomposed as

$$\mu_x^G = \mu_x^G \lfloor_{B_{\mathcal{M}}(x, \varepsilon')} + \mu_x^G \lfloor_{B_G(x, \varepsilon) \setminus B_{\mathcal{M}}(x, \varepsilon')},$$

where now $\varepsilon' := \varepsilon - 3W_\infty(\mu, \mu_n) - C_1\beta\varepsilon^3 - (C_2 + C'_{\mathcal{M}})\varepsilon^4$ and, we recall, B_G is as in (51). Notice that the additional terms in the definition of ε' , relative to how ε' was defined in the proof of Theorem 10, account for the discrepancy between $d_{\mathcal{M}}$ and \hat{d}_g . With this definition we have $B_{\mathcal{M}}(x, \varepsilon') \cap \mathcal{X} \subseteq B_G(x, \varepsilon)$.

We define the measure $\mu_{y,1}^G$ as

$$\mu_{y,1}^G := aT_{n\sharp}(\mathcal{F}_\sharp(\mu_x^{\mathcal{M}} \lfloor_{T_n^{-1}(B_{\mathcal{M}}(x, \varepsilon'))})),$$

for T_n, \mathcal{F} and $\mu_x^{\mathcal{M}}$ as in Case 2 in the proof of Theorem 10. We can follow the same steps there to conclude that $\mu_{y,1}^G \leq \mu_y^G$ and then define $\mu_{y,2}^G := \mu_y^G - \mu_{y,1}^G$. Also, we may introduce analogous couplings Π and $\pi_1^G = T_{1,4\sharp}\Pi \in \Gamma(\mu_x^G \lfloor_{B_{\mathcal{M}}(x, \varepsilon')}, \mu_{y,1}^G)$ for which:

$$d_{\mathcal{M}}(\tilde{x}, \tilde{y}) = d_{\mathcal{M}}(x, y) \left(1 - d_{\mathcal{M}}(x, \tilde{x}')^2 \left(\frac{K(v, w')}{2} + O(d_{\mathcal{M}}(x, y) + \varepsilon) \right) \right) + O(W_\infty(\mu, \mu_n))$$

for all $(\tilde{x}, \tilde{x}', \tilde{y}', \tilde{y}) \in \text{spt}(\Pi)$. In turn, we can use the approximation error estimates for $\hat{d}_g - d_{\mathcal{M}}$ to obtain

$$\hat{d}_g(\tilde{x}, \tilde{y}) = \hat{d}_g(x, y) \left(1 - d_{\mathcal{M}}(x, \tilde{x}')^2 \left(\frac{K(v, w')}{2} + O(\hat{d}_g(x, y) + \varepsilon) \right) \right) + O(\beta\varepsilon^3 + \varepsilon^4 + W_\infty(\mu, \mu_n))$$

for all $(\tilde{x}, \tilde{x}', \tilde{y}', \tilde{y}) \in \text{spt}(\Pi)$, and $d_{G,\mathcal{X}}(\tilde{x}, \tilde{y}) \leq \tilde{d}_{G,\mathcal{X}}(\tilde{x}, \tilde{y}) = \delta_0 \psi(\hat{d}_g(x, y)/\delta_0)$ for all $(\tilde{x}, \tilde{y}) \in \text{spt}(\pi_1^G)$. From this we can conclude that

$$\begin{aligned} W_{1,G}(\mu_x^G \llcorner_{B_{\mathcal{M}}(x,\varepsilon')}, \mu_{y,1}^G) &\leq \int d_{G,\mathcal{X}}(\tilde{x}, \tilde{y}) d\pi_1^G(\tilde{x}, \tilde{y}) = \int d_{G,\mathcal{X}}(\tilde{x}, \tilde{y}) d\Pi(\tilde{x}, \tilde{x}', \tilde{y}', \tilde{y}) \\ &\leq \delta_0 \psi(\hat{d}_g(x, y)/\delta_0) - \psi' \left(\frac{\hat{d}_g(x, y)}{\delta_0} \right) \hat{d}_g(x, y) \varepsilon^2 \frac{\text{Ric}_x(v)}{2(m+2)} \\ &\quad + C(\beta \varepsilon^3 + \varepsilon^4 + W_\infty(\mu, \mu_n)). \end{aligned} \tag{52}$$

In addition,

$$\begin{aligned} W_{1,G}(\mu_x^G \llcorner_{B_{\mathcal{M}}(x,\varepsilon) \setminus B_{\mathcal{M}}(x,\varepsilon')}, \mu_{y,2}^G) &\leq C\varepsilon \frac{\mu_n(B_{\mathcal{M}}(x,\varepsilon) \setminus B_{\mathcal{M}}(x,\varepsilon'))}{\mu_n(B_{\mathcal{M}}(x,\varepsilon))} \\ &\leq C(W_\infty(\mu, \mu_n) + \beta \varepsilon^3 + \varepsilon^4), \end{aligned}$$

thanks to Lemma 4.

We may now invoke Lemma 3 and (52) to get

$$\begin{aligned} W_{1,G}(\mu_x^G, \mu_y^G) &\leq W_{1,G}(\mu_x^G \llcorner_{B_{\mathcal{M}}(x,\varepsilon')}, \mu_{y,1}^G) + W_{1,G}(\mu_x^G \llcorner_{B_{\mathcal{M}}(x,\varepsilon) \setminus B_{\mathcal{M}}(x,\varepsilon')}, \mu_{y,2}^G) \\ &\leq \delta_0 \psi(\hat{d}_g(x, y)/\delta_0) - \psi' \left(\frac{\hat{d}_g(x, y)}{\delta_0} \right) \hat{d}_g(x, y) \varepsilon^2 \frac{\text{Ric}_x(v)}{2(m+2)} \\ &\quad + C(\beta \varepsilon^3 + \varepsilon^4 + W_\infty(\mu, \mu_n)). \end{aligned} \tag{53}$$

Recalling that $d_{G,\mathcal{X}}(x, y) = \delta_0 \psi(\hat{d}_g(x, y)/\delta_0) \geq \delta_0 \psi(0) = c_0 \psi(0) \varepsilon$, we deduce

$$\begin{aligned} \frac{\kappa_G(x, y)}{\varepsilon^2} &= \frac{1}{\varepsilon^2} \left(1 - \frac{W_{1,G}(\mu_x^G, \mu_y^G)}{d_{G,\mathcal{X}}(x, y)} \right) \geq \psi' \left(\frac{\hat{d}_g(x, y)}{\delta_0} \right) \frac{\hat{d}_g(x, y)}{\delta_0 \psi \left(\frac{\hat{d}_g(x, y)}{\delta_0} \right)} \frac{\text{Ric}_x(v)}{2(m+2)} \\ &\quad - C \left(\beta + \varepsilon + \frac{W_\infty(\mu, \mu_n)}{\varepsilon^3} \right). \end{aligned} \tag{54}$$

The lower bound (34) now follows.

Case 3: Here we assume that $\delta_1 - 2\varepsilon \leq \hat{d}_g(x, y) \leq \delta_1$.

As in Case 3 in the proof of Theorem 10 we consider the midpoint \bar{x} between x and y (along the manifold geodesic). It is straightforward to see from 1 in Assumption 1 that

$$\left| \frac{\hat{d}_g(\bar{x}, y)}{\hat{d}_g(x, y)} - \frac{1}{2} \right| \leq C\beta \varepsilon^2 + C\varepsilon^3, \quad \left| \frac{\hat{d}_g(\bar{x}, x)}{\hat{d}_g(x, y)} - \frac{1}{2} \right| \leq C\beta \varepsilon^2 + C\varepsilon^3. \tag{55}$$

Then

$$\begin{aligned}
\kappa_G(x, y) &\geq 1 - \frac{W_{1,G}(\mu_x^G, \mu_{\bar{x}}^G) + W_{1,G}(\mu_{\bar{x}}^G, \mu_y^G)}{d_{G,\mathcal{X}}(x, y)} \\
&= 1 - \frac{W_{1,G}(\mu_x^G, \mu_{\bar{x}}^G) + W_{1,G}(\mu_{\bar{x}}^G, \mu_y^G)}{\hat{d}_g(x, y)} \\
&\geq \frac{\hat{d}_g(x, \bar{x})}{\hat{d}_g(x, y)} \left(1 - \frac{W_{1,G}(\mu_x^G, \mu_{\bar{x}}^G)}{\hat{d}_g(x, \bar{x})} \right) + \frac{\hat{d}_g(\bar{x}, y)}{\hat{d}_g(x, y)} \left(1 - \frac{W_{1,G}(\mu_{\bar{x}}^G, \mu_y^G)}{\hat{d}_g(\bar{x}, y)} \right) \\
&\quad - C\beta\varepsilon^2 - C\varepsilon^3.
\end{aligned}$$

As in the proof of Theorem 10, we may now use (54) to bound from below each of the terms $\left(1 - \frac{W_{1,G}(\mu_x^G, \mu_{\bar{x}}^G)}{\hat{d}_g(x, \bar{x})}\right)$ and $\left(1 - \frac{W_{1,G}(\mu_{\bar{x}}^G, \mu_y^G)}{\hat{d}_g(\bar{x}, y)}\right)$ by $\frac{1}{2}(s_K\varepsilon^2K - C(\beta\varepsilon^2 + \varepsilon^3 + \frac{W_\infty(\mu, \mu_n)}{\varepsilon}))$. \square

Remark 18. In the regime $\hat{d}_g(x, y) \sim \varepsilon$, i.e., the regime corresponding to Case 2 in the proof of Theorem 13, we use the fact that \hat{d}_g satisfies

$$\hat{d}_g(x, y) = d_{\mathcal{M}}(x, y) + O(\beta\varepsilon^3 + \varepsilon^4),$$

whereas an approximation error of order $O(\varepsilon^3)$ would have produced a lower bound on discrete curvature of the form $s_KK - C$ for some constant C that may be larger than s_KK itself. In particular, if the error was of order $O(\varepsilon^3)$, the sign of the discrete lower bound would not be guaranteed to be consistent with the sign of the manifold's curvature lower bound. From our proof it thus seems that $\hat{d}_g(x, y)$ cannot be simply taken to be the Euclidean distance between x and y and a finer estimator seems to be necessary.

6.3 Pointwise consistency

Next, we present the proof of our pointwise consistency results, i.e., Theorems 8 and 9.

Proof of Theorem 8. Since $d_{\mathcal{M}}(x, y)$ is assumed to satisfy $2\delta_0 \leq d_{\mathcal{M}}(x, y) \leq \frac{1}{2}\delta_1$, we may use Proposition 2, (50) in Case 2 in the proof of Theorem 10, and the fact that $\psi(t) = t$ for $t \geq 1$ to conclude that

$$\frac{\kappa_G(x, y)}{\varepsilon^2} \geq \frac{\text{Ric}_x(v)}{2(m+2)} - C \left(\varepsilon + \frac{W_\infty(\mu, \mu_n)}{\varepsilon^3} \right).$$

It thus remains to obtain matching upper bounds.

For this purpose, let $f : \mathcal{M} \rightarrow \mathbb{R}$ be the function defined in (44). Using (26) in Proposition 2 and the fact that f is 1-Lipschitz with respect to $d_{\mathcal{M}}$, we conclude that the function f restricted to \mathcal{X} is 1-Lipschitz with respect to $d_{G,\mathcal{M}}$.

In turn, thanks to the Kantorovich-Rubinstein theorem (i.e., Theorem 14) we obtain

$$\int f(\tilde{y})d\mu_y^G(\tilde{y}) - \int f(\tilde{x})d\mu_x^G(\tilde{x}) \leq W_{1,G}(\mu_x^G, \mu_y^G).$$

Using again the fact that f is 1-Lipschitz with respect to $d_{\mathcal{M}}$ we deduce

$$\left| \int f(\tilde{x})d\mu_x^G(\tilde{x}) - \int f(\tilde{x})d\mu_x^{\mathcal{M}}(\tilde{x}) \right| \leq W_1(\mu_x^G, \mu_x^{\mathcal{M}}),$$

and

$$\left| \int f(\tilde{x})d\mu_y^G(\tilde{y}) - \int f(\tilde{y})d\mu_y^{\mathcal{M}}(\tilde{y}) \right| \leq W_1(\mu_y^G, \mu_y^{\mathcal{M}}).$$

Putting together the above inequalities we conclude that

$$\int f(\tilde{y})d\mu_y^{\mathcal{M}}(\tilde{y}) - \int f(\tilde{x})d\mu_x^{\mathcal{M}}(\tilde{x}) \leq W_{1,G}(\mu_x^G, \mu_y^G) + W_1(\mu_x^G, \mu_x^{\mathcal{M}}) + W_1(\mu_y^G, \mu_y^{\mathcal{M}}).$$

Using now (46), we can lower bound the left hand side of the above expression and conclude that

$$1 - \varepsilon^2 \frac{\text{Ric}_x(v)}{2(m+2)} \leq \frac{W_{1,G}(\mu_x^G, \mu_y^G)}{d_{\mathcal{M}}(x, y)} + \varphi, \quad (56)$$

where

$$\varphi := C(d_{\mathcal{M}}(x, y)\varepsilon^2 + \varepsilon^3) + \frac{W_1(\mu_x^G, \mu_x^{\mathcal{M}})}{d_{\mathcal{M}}(x, y)} + \frac{W_1(\mu_y^G, \mu_y^{\mathcal{M}})}{d_{\mathcal{M}}(x, y)}.$$

Using the fact that $d_{G,\mathcal{M}}(x, y) = d_{\mathcal{M}}(x, y)$ by Proposition 2, and rearranging terms, we conclude that

$$\kappa_G(x, y) \leq \varepsilon^2 \frac{\text{Ric}_x(v)}{2(m+2)} + C(d_{\mathcal{M}}(x, y)\varepsilon^2 + \varepsilon^3) + \frac{W_1(\mu_x^G, \mu_x^{\mathcal{M}})}{d_{\mathcal{M}}(x, y)} + \frac{W_1(\mu_y^G, \mu_y^{\mathcal{M}})}{d_{\mathcal{M}}(x, y)}.$$

To finish the proof, it remains to notice that the terms $W_1(\mu_x^G, \mu_x^{\mathcal{M}})$ and $W_1(\mu_y^G, \mu_y^{\mathcal{M}})$ can be bounded above by $CW_{\infty}(\mu, \mu_n)$, as it follows easily from an application of Lemma 4. □

Proof of Theorem 9. From Case 2 in the proof of Theorem 13 we have

$$\frac{\kappa_G(x, y)}{\varepsilon^2} \geq \frac{\text{Ric}_x(v)}{2(m+2)} - C \left(\beta + \varepsilon + \frac{W_{\infty}(\mu, \mu_n)}{\varepsilon^3} \right),$$

and thus it remains to obtain a matching upper bound.

First of all, notice that, thanks to (16) and Assumption 3, we can assume that $2\delta_0 \leq d_{\mathcal{M}}(x, y) \leq \frac{\delta_1}{2}$. Now, from (27) and (28) in Proposition 2 we have

$$\left| \frac{d_{\mathcal{M}}(x, y)}{d_{G,\mathcal{X}}(x, y)} - 1 \right| \leq C(\beta\varepsilon^2 + \varepsilon^3). \quad (57)$$

On the other hand, thanks to (27), it follows that the function f from (44) restricted to \mathcal{X} has Lipschitz constant, with respect to $d_{G,\mathcal{X}}$, no larger than $1 + C(\beta\varepsilon^2 + \varepsilon^3)$. This implies that

$$\int f(\tilde{y})d\mu_y^G(\tilde{y}) - \int f(\tilde{x})d\mu_x^G(\tilde{x}) \leq (1 + C(\beta\varepsilon^2 + \varepsilon^3))W_{1,G}(\mu_x^G, \mu_y^G).$$

Proceeding as in the proof of Theorem 8 we can conclude that

$$1 - \varepsilon^2 \frac{\text{Ric}_x(v)}{2(m+2)} \leq (1 + C(\beta\varepsilon^2 + \varepsilon^3)) \frac{W_{1,G}(\mu_x^G, \mu_y^G)}{d_{\mathcal{M}}(x, y)} + \varphi,$$

for φ as in (56). In turn, multiplying both sides of the above by $\frac{1}{1+C(\beta\varepsilon^2+\varepsilon^3)} \frac{d_{\mathcal{M}}(x,y)}{d_{G,\mathcal{X}}(x,y)}$, using (57), and rearranging terms, we conclude that

$$\kappa_G(x, y) \leq \varepsilon^2 \frac{\text{Ric}_x(v)}{2(m+2)} + C(\beta\varepsilon^2 + \varepsilon^3) + \frac{W_1(\mu_x^G, \mu_x^{\mathcal{M}})}{d_{\mathcal{M}}(x, y)} + \frac{W_1(\mu_y^G, \mu_y^{\mathcal{M}})}{d_{\mathcal{M}}(x, y)}.$$

The result now follows from the fact that, thanks to (16) and Lemma (4), each of the terms $W_1(\mu_x^G, \mu_x^{\mathcal{M}})$ and $W_1(\mu_y^G, \mu_y^{\mathcal{M}})$ is bounded by $C(W_\infty(\mu, \mu_n) + \beta\varepsilon^3 + \varepsilon^4)$. \square

7 Applications

7.1 Lipschitz contractivity of the graph heat kernel

In this section we discuss some of the implications of our curvature lower bounds on the heat kernel associated to the *unnormalized graph Laplacian* Δ_n induced by the graph $G = (\mathcal{X}, w_\varepsilon)$. We recall that the unnormalized graph Laplacian associated to G is defined as

$$\Delta_n u(x) := \frac{1}{n\varepsilon^{m+2}} \sum_{\tilde{x} \in \mathcal{X}} \omega_\varepsilon(x, \tilde{x})(u(x) - u(\tilde{x})), \quad u \in L^2(\mathcal{X}). \quad (58)$$

We will focus on the choice $w_\varepsilon = w_{\varepsilon, \mathcal{M}}$ (see (10)) for simplicity, but we remark that a lot of the discussion presented below can be adapted to the choice $w_\varepsilon = w_{\varepsilon, \mathcal{X}}$.

Remark 19. *The operator Δ_n can be written in matrix form as*

$$\Delta_n = \frac{1}{\varepsilon^2}(D - W),$$

where W is the weight matrix induced by the rescaled weights $\frac{1}{n\varepsilon^m}w_\varepsilon$ and D is the degree matrix associated to W .

Δ_n plays a central role in graph-based learning, where it is used to define algorithms for supervised, semi-supervised, and unsupervised learning; see, e.g., [2, 34, 47] for some discussion. There are several results in the literature that discuss the asymptotic convergence of Δ_n toward \mathcal{M} 's Laplace-Beltrami operator; see e.g. [24] for pointwise convergence and [6, 8, 9, 15, 22, 51] for spectral convergence. Here we add upon the existing literature on graph Laplacians by providing novel contraction results that are implied by our curvature lower bounds. Specifically, we are interested in the behavior of the heat operator $e^{-t\Delta_n}$ as $t \rightarrow \infty$. The heat operator $e^{-t\Delta_n}$ can be defined via the spectral theorem or as the operator mapping an initial condition $u \in L^2(\mathcal{X})$ to the solution at time t of the graph heat equation:

$$\begin{cases} \partial_s u_s = -\Delta_n u_s, \\ u_0 = u. \end{cases} \quad (59)$$

In what follows we abuse notation slightly and use $D(x)$ to denote the degree of $x \in \mathcal{X}$. Precisely,

$$D(x) := \frac{1}{n\varepsilon^m} \sum_{y \in \mathcal{X}} \eta\left(\frac{d_{\mathcal{M}}(x, y)}{\varepsilon}\right),$$

where $\eta(t) := \mathbb{1}_{t \leq 1}$. D can be thought of as a kernel density estimator for the distribution used to sample the data set \mathcal{X} , in this case the uniform measure over \mathcal{M} . Precisely, one can show via standard concentration arguments that for every $r \in [\varepsilon^2, 1]$ we have

$$\max_{x \in \mathcal{X}} |\alpha_{\mathcal{M}} - D(x)| \leq Cr, \quad (60)$$

with probability at least $1 - c(r\varepsilon)^{-m} \exp(-cr^2 n\varepsilon^m)$; e.g., see Corollary 3.7 in [8] for a closely related estimate. In the above, $\alpha_{\mathcal{M}} \text{vol}(\mathcal{M})$ is the volume of the m -dimensional Euclidean unit ball.

We study the evolution, along the heat flow, of the Lipschitz seminorm of a function $u : \mathcal{X} \rightarrow \mathbb{R}$ when \mathcal{X} is endowed with the distance $d_G = d_{G, \mathcal{M}}$. This seminorm is defined as:

$$\text{Lip}_G(u) := \max_{x, y \in \mathcal{X}, x \neq y} \frac{|u(x) - u(y)|}{d_G(x, y)}. \quad (61)$$

Lemma 6. *For a given $u : \mathcal{X} \rightarrow \mathbb{R}$ let*

$$\mathcal{A}u(x) := \int u(\tilde{x}) d\mu_x^G(\tilde{x}) = \frac{1}{n\varepsilon^m D(x)} \sum_{z \in \mathcal{X}} w_\varepsilon(x, z) u(z), \quad x \in \mathcal{X}.$$

Under the same assumptions as in Theorem 10 it follows that

$$\text{Lip}_G(\mathcal{A}u) \leq (1 - \varepsilon^2 K_G) \text{Lip}_G(u), \quad \forall u \in L^2(\mathcal{X}),$$

where

$$K_G := \min \left\{ s_K K - C \left(\varepsilon + \frac{W_\infty(\mu, \mu_n)}{\varepsilon^3} \right), \frac{1}{2\varepsilon^2} \right\}.$$

Proof. This is an immediate consequence of the definition of Ollivier Ricci curvature and the dual representation of the 1-Wasserstein distance. Indeed, by Theorem 10 and the Kantorovich-Rubinstein theorem, for all $x, y \in \mathcal{X}$ we have

$$\begin{aligned} (1 - \varepsilon^2 K_G) d_G(x, y) &\geq W_1(\mu_x^G, \mu_y^G) \geq \frac{1}{\text{Lip}_G(u)} \left(\int u(\tilde{x}) d\mu_x^G(\tilde{x}) - \int u(\tilde{y}) d\mu_y^G(\tilde{y}) \right) \\ &= \frac{1}{\text{Lip}_G(u)} (\mathcal{A}u(x) - \mathcal{A}u(y)). \end{aligned}$$

Since the above is true for all $x, y \in \mathcal{X}$ we obtain the desired result. \square

Using Lemma 6 we can establish the following contraction of Lip_G along the heat flow $e^{-t\Delta_n}$.

Theorem 20. *Under the same assumptions as in Theorem 10, and letting K_G be defined as in Lemma 6, for all $u : \mathcal{X} \rightarrow \mathbb{R}$ we have*

$$\text{Lip}_G(e^{-t\Delta_n} u) \leq \exp \left(- \left(K_G - \frac{4\|D - \alpha_{\mathcal{M}}\|_{L^\infty(\mathcal{X})} \text{diam}(G)}{c_0 \psi(0) \varepsilon^3} \right) t \right) \text{Lip}_G(u), \quad (62)$$

where $\text{diam}(G) := \max_{x, y \in \mathcal{X}} d_G(x, y)$.

Proof. We start by noticing that inequality (62) is invariant under addition of constants. This is because $e^{-t\Delta_n}(u+c) = e^{-t\Delta_n}u + c$. Due to this, from now on we can assume without the loss of generality that u is such that $\sum_{z \in \mathcal{X}} u(z) = 0$.

Now, fix $t \in [0, \infty)$ and let $x, y \in \mathcal{X}$ be a pair of data points such that

$$\frac{e^{-t\Delta_n} u(x) - e^{-t\Delta_n} u(y)}{d_G(x, y)} = \text{Lip}_G(e^{-t\Delta_n} u);$$

such pair always exists because \mathcal{X} is a finite set. Notice that

$$\frac{d}{dt} \frac{(e^{-t\Delta_n} u(x) - e^{-t\Delta_n} u(y))^2}{2d_G(x, y)^2} = \frac{e^{-t\Delta_n} u(x) - e^{-t\Delta_n} u(y)}{d_G(x, y)^2} \cdot (-\Delta_n e^{-t\Delta_n} u(x) + \Delta_n e^{-t\Delta_n} u(y)). \quad (63)$$

We rewrite the term $\Delta_n e^{-t\Delta_n} u(x)$ as

$$\begin{aligned} \frac{1}{\varepsilon^2} D(x) e^{-t\Delta_n} u(x) - \frac{1}{n\varepsilon^{m+2}} \sum_{z \in \mathcal{X}} w_\varepsilon(x, z) e^{-t\Delta_n} u(z) &= \frac{\alpha_{\mathcal{M}}}{\varepsilon^2} e^{-t\Delta_n} u(x) - \frac{\alpha_{\mathcal{M}}}{\varepsilon^2} \mathcal{A}e^{-t\Delta_n} u(x) \\ &+ \frac{1}{\varepsilon^2} (D(x) - \alpha_{\mathcal{M}}) e^{-t\Delta_n} u(x) \\ &+ \frac{1}{n\varepsilon^{m+2}} \left(\frac{\alpha_{\mathcal{M}} - D(x)}{D(x)} \right) \sum_{z \in \mathcal{X}} w_\varepsilon(x, z) e^{-t\Delta_n} u(z). \end{aligned}$$

We plug this expression (and the one corresponding to $\Delta_n e^{-t\Delta_n} u(y)$) in (63) to

conclude that

$$\begin{aligned}
\frac{d}{dt} \frac{(e^{-t\Delta_n}u(x) - e^{-t\Delta_n}u(y))^2}{2d_G(x,y)^2} &\leq -\alpha_{\mathcal{M}} \frac{(e^{-t\Delta_n}u(x) - e^{-t\Delta_n}u(y))^2}{\varepsilon^2 d_G(x,y)^2} + \frac{\alpha_{\mathcal{M}}}{\varepsilon^2} \text{Lip}_G(e^{-t\Delta_n}u) \text{Lip}_G(\mathcal{A}e^{-t\Delta_n}u) \\
&+ \frac{4}{\varepsilon^2 \delta_0 \psi(0)} \text{Lip}_G(e^{-t\Delta_n}u) \|D - \alpha_{\mathcal{M}}\|_{L^\infty(\mathcal{X})} \|e^{-t\Delta_n}u\|_{L^\infty(\mathcal{X})} \\
&\leq -\frac{\alpha_{\mathcal{M}} (\text{Lip}_G(e^{-t\Delta_n}u))^2}{\varepsilon^2} + \frac{\alpha_{\mathcal{M}}}{\varepsilon^2} (1 - \varepsilon^2 K_G) (\text{Lip}_G(e^{-t\Delta_n}u))^2 \\
&+ \frac{4}{\varepsilon^2 \delta_0 \psi(0)} \text{Lip}_G(e^{-t\Delta_n}u) \|D - \alpha_{\mathcal{M}}\|_{L^\infty(\mathcal{X})} \|e^{-t\Delta_n}u\|_{L^\infty(\mathcal{X})},
\end{aligned}$$

where in the second inequality we have used Corollary 6. By assumption we have $\frac{1}{n} \sum_{z \in \mathcal{X}} e^{-t\Delta_n}u(z) = \frac{1}{n} \sum_{z \in \mathcal{X}} u(z) = 0$ and thus it follows

$$|e^{-t\Delta_n}u(z')| = \left| \frac{1}{n} \sum_{z \in \mathcal{X}} (e^{-t\Delta_n}u(z') - e^{-t\Delta_n}u(z)) \right| \leq \text{diam}(G) \cdot \text{Lip}_G(e^{-t\Delta_n}u),$$

for every $z' \in \mathcal{X}$. This allows us to bound $\|e^{-t\Delta_n}u\|_{L^\infty(\mathcal{X})} \leq \text{diam}(G) \cdot \text{Lip}_G(e^{-t\Delta_n}u)$. Hence

$$\frac{d}{dt} \frac{(e^{-t\Delta_n}u(x) - e^{-t\Delta_n}u(y))^2}{d_G(x,y)^2} \leq -2 \left(\alpha_{\mathcal{M}} K_G - \frac{4 \|D - \alpha_{\mathcal{M}}\|_{L^\infty(\mathcal{X})} \text{diam}(G)}{\varepsilon^2 \delta_0 \psi(0)} \right) (\text{Lip}_G(e^{-t\Delta_n}u))^2.$$

Since (x, y) was an arbitrary pair realizing $\text{Lip}_G(e^{-t\Delta_n}u)$ we conclude that

$$\frac{d}{dt} (\text{Lip}_G(e^{-t\Delta_n}u))^2 \leq -2 \left(\alpha_{\mathcal{M}} K_G - \frac{4 \|D - \alpha_{\mathcal{M}}\|_{L^\infty(\mathcal{X})} \text{diam}(G)}{\varepsilon^2 \delta_0 \psi(0)} \right) (\text{Lip}_G(e^{-t\Delta_n}u))^2.$$

Gronwall's inequality implies that

$$(\text{Lip}_G(e^{-t\Delta_n}u))^2 \leq \exp \left(-2 \left(\alpha_{\mathcal{M}} K_G - \frac{4 \|D - \alpha_{\mathcal{M}}\|_{L^\infty(\mathcal{X})} \text{diam}(G)}{\varepsilon^2 \delta_0 \psi(0)} \right) t \right) (\text{Lip}_G(u))^2.$$

Taking square roots on both sides we obtain the desired result. \square

Remark 21. *In order for the exponent on the right hand side of (62) to be negative, we certainly need K_G to be strictly positive, which we can guarantee when \mathcal{M} is a manifold with Ricci curvature bounded from below by a positive quantity and the assumptions of Theorem 10 are satisfied. We also need to make sure that the quantity $\frac{\|D - \alpha_{\mathcal{M}}\|_{L^\infty(\mathcal{X})}}{\varepsilon^3}$ is sufficiently small, which is implied by the assumptions in Theorem 10 and the bound (60). The bottom line is that, when \mathcal{X} is sampled from a manifold with positive Ricci curvature, then, under the assumptions in Theorem 10, for all large enough n the Lipschitz seminorm Lip_G contracts along the heat flow associated to the unnormalized Laplacian for the graph $G = (\mathcal{X}, w_{\varepsilon, \mathcal{M}})$.*

Remark 22. We emphasize that Δ_n in Theorem 20 is the unnormalized Laplacian of $G = (\mathcal{X}, w_{\varepsilon, \mathcal{M}})$, which we recall depends on the geodesic distance over \mathcal{M} . While our curvature lower bound results do not allow us to say anything about Laplacians for RGGs with the Euclidean distance, one can certainly deduce adaptations of Theorem 20 for proximity graphs built from slight modifications of the Euclidean distance. In particular, it is clear that a similar statement can be derived, *mutatis mutandis*, for the graph $G = (\mathcal{X}, w_{\varepsilon, \mathcal{X}})$ endowed with distance $d_{G, \mathcal{X}}$.

Remark 23. To contrast the content of Theorem 20 with other contractivity results known in the literature, let λ_G be the first nontrivial eigenvalue of Δ_n . Using the spectral theorem one can easily show that for all $u \in L^2(\mathcal{X})$

$$\|e^{-t\Delta_n}u - \bar{u}\|_{L^2(\mathcal{X})}^2 \leq e^{-t\lambda_G} \|u - \bar{u}\|_{L^2(\mathcal{X})}^2,$$

where $\bar{u} = \frac{1}{n} \sum_{z \in \mathcal{X}} u(z)$. Spectral consistency results for Δ_n like the ones in [6, 8, 9, 15, 22, 51] guarantee that λ_G does not deteriorate as the graph G is scaled up. Naturally, from these L^2 contraction estimates one can not derive Lipschitz contraction as in Theorem 20 and our results in this paper thus provide novel results for the literature of graph Laplacians on data clouds. It is worth highlighting, however, that for $\lambda_G > 0$ to remain bounded away from zero, one does not require \mathcal{M} 's Ricci curvature to be positive.

Remark 24. In the literature on graph based learning it is not unusual to replace a graph Laplacian with a version of it that is obtained by truncating its spectral decomposition, which in particular requires the use of an eigensolver. We emphasize that Theorem 20 and its Corollary 2 below is a structural property that holds for the full Laplacian Δ_n and not for a truncation thereof.

An immediate consequence of Theorem 20 is the following.

Corollary 2. Under the same assumptions as in Theorem 20 we have

$$\|e^{-t\Delta_n}u - \bar{u}\|_{L^\infty(\mathcal{X})} \leq \exp\left(-\left(K_G - \frac{4\|D - \alpha_{\mathcal{M}}\|_{L^\infty(\mathcal{X})}\text{diam}(G)}{c_0\psi(0)\varepsilon^3}\right)t\right) \text{diam}(G)\text{Lip}_G(u),$$

where $\bar{u} := \frac{1}{n} \sum_{x \in \mathcal{X}} u(x)$.

Proof. Notice that for any function $v : \mathcal{X} \rightarrow \mathbb{R}$ and any $x \in \mathcal{X}$ we have

$$|v(x) - \bar{v}| = \left| \frac{1}{n} \sum_{\tilde{x} \in \mathcal{X}} (v(x) - v(\tilde{x})) \right| \leq \text{diam}(G)\text{Lip}(v),$$

from where it follows that

$$\|v - \bar{v}\|_{L^\infty(\mathcal{X})} \leq \text{diam}(G)\text{Lip}_G(v).$$

The result now follows from Theorem 20. □

7.2 Manifold Learning

We briefly comment on another class of estimation problems on point clouds and graphs where curvature lower bounds may be utilized.

Recognizing and characterizing geometric structure in data is a cornerstone of Representation Learning. A common assumption is that the data lies on or near a low-dimensional manifold $\mathcal{M} \subseteq \mathbb{R}^d$ (*manifold hypothesis*). Suppose we are given a point cloud $\mathcal{X} \subseteq \mathbb{R}^d$ in a high-dimensional Euclidean space, i.e., our data was sampled from an embedded manifold and we have access to pairwise Euclidean distances between data points. What can we learn about the dimension and curvature of \mathcal{M} given only pairwise Euclidean distances in \mathcal{X} ? A rich body of literature has considered this question from different angles. Several algorithms exist for inferring the *intrinsic dimension* of \mathcal{X} (i.e., $\dim(\mathcal{M})$). However, such algorithms do not allow inference on intrinsic geometric quantities of \mathcal{M} such as a global curvature bound. There are several approaches for approximating *extrinsic* curvature, some of which were reviewed in earlier sections of this paper. However, none of these techniques allow for learning the *intrinsic* curvature of the manifold. The consistency results developed in this paper allow for such inference, even in the case where one has only access to data-driven estimates of pairwise geodesic distances, as is usually the case in practise.

Manifold learning aims to identify a putative manifold $\widetilde{\mathcal{M}} \subseteq \mathbb{R}^d$ whose geometry agrees with the low-dimensional structure in \mathcal{X} . That is, one learns a point configuration $\phi(\mathcal{X})$, which is the output of an implicit map $\phi : \mathcal{X} \rightarrow \widetilde{\mathcal{M}}$, that approximately preserves the pairwise distances ($d_{\mathcal{X}}(x, y) \approx d_{\widetilde{\mathcal{M}}}(\phi(x), \phi(y))$ for all $x, y \in \mathcal{X}$). A large number of algorithms has been proposed for this task, including Isomap [42], Laplacian Eigenmaps [2] and Locally Linear Embeddings [39]. While these algorithms have gained popularity in practice, it is often challenging to certify that the geometry of the putative manifold $\widetilde{\mathcal{M}}$ aligns with that of the true manifold \mathcal{M} . To the best of our knowledge, the strongest guarantees are available for Isomap, which is known to recover the intrinsic dimension, as well as, asymptotically, the pairwise distances, in the large-sample limit [3]. However, none of these manifold learning algorithms are guaranteed to recover global curvature bounds. The consistency of global curvature bounds (Theorems 13) provides an effective, unsupervised means for testing whether \mathcal{M} has a curvature lower bound by computing Ollivier’s Ricci curvature on a geometric graph constructed from \mathcal{X} . The resulting tool, complementary to standard manifold learning techniques, could allow for learning a more comprehensive geometric characterization of a given point cloud. Curvature lower bounds may also serve as inductive biases in manifold learning approaches. The choice of manifold learning technique often requires prior knowledge on the type of manifold that is to be learnt, e.g., if the data was sampled from a linear subspace, a linear method, such as Principal Component Analysis, is suitable. On the other hand, if the data is sampled from a nonlinear subspace, such as an embedded submanifold, a nonlinear approach, such as Isomap, is expected to perform better.

8 Conclusions

In this paper, we have investigated continuum limits of Ollivier’s Ricci curvature on random geometric graphs in the sense of local pointwise consistency and in the sense of global lower bounds. Specifically, we consider a data cloud \mathcal{X} sampled uniformly from a low-dimensional manifold $\mathcal{M} \subseteq \mathbb{R}^d$. We construct a proximity graph G of \mathcal{X} that allows us to give non-asymptotic error bounds for the approximation of \mathcal{M} ’s curvature from data. Moreover, we show that if \mathcal{M} has curvature bounded below by a positive constant, then so does G with high probability. To the best of our knowledge, our local consistency result presents the first *non-asymptotic* guarantees of this kind. In addition, we believe that our work provides the first consistency results for global curvature bounds. We complement our theoretical investigation of continuum limits with a discussion of potential applications to manifold learning.

We conclude with a brief discussion of avenues for future investigation. A limitation of the present work is the assumption that \mathcal{X} is a uniform sample. Future work may investigate whether it is possible to adapt these results to other data distributions. Furthermore, we have assumed that the sample is noise-free; it would be interesting to analyze the noisy case with different noise models. In addition, one setting investigated in this work implicitly assumes access to a sufficiently good data-driven estimator for the geodesic distance. While we have suggested some directions for constructing such estimator, we believe that this question is of interest in its own right and deserves more attention. We would also like to highlight the “shrinking” factor s_K that appears in our main Theorems 10 and 13 should be removable with a much more detailed analysis. Further applications of the global curvature lower bounds may arise in the study of Langevin dynamics on manifolds, specifically when utilizing graph-based constructions to define suitable discretizations of the infinitesimal generators of the stochastic dynamics of interest.

Acknowledgements

The authors would like to thank Prasad Tetali for enlightening discussions and for providing relevant references. This work was started while the authors were visiting the Simons Institute to participate in the program “Geometric Methods in Optimization and Sampling” during the Fall of 2021. The authors would like to thank the organizers of this program and the Simons Institute for support and hospitality. During the visit, MW was supported by a Simons-Berkeley Research Fellowship. NGT was supported by NSF-DMS grant 2005797 and would also like to thank the IFDS at UW-Madison and NSF through TRIPODS grant 2023239 for their support.

References

- [1] Eddie Aamari and Clément Levrard. Nonasymptotic rates for manifold, tangent space and curvature estimation. *The Annals of Statistics*, 47(1):177–204, February 2019. Publisher: Institute of Mathematical Statistics.
- [2] Mikhail Belkin and Partha Niyogi. Laplacian eigenmaps for dimensionality reduction and data representation. *Neural computation*, 15(6):1373–1396, 2003.
- [3] Mira Bernstein, Vin De Silva, John C Langford, and Joshua B Tenenbaum. Graph approximations to geodesics on embedded manifolds. Technical report, 2000.
- [4] Nicolas Boumal. An introduction to optimization on smooth manifolds.
- [5] Leon Bungert, Jeff Calder, and Tim Roith. Uniform convergence rates for lipschitz learning on graphs. *IMA Journal of Numerical Analysis*, September 2022.
- [6] Dmitri Burago, Sergei Ivanov, and Yaroslav Kurylev. A graph discretization of the laplace–beltrami operator. *Journal of Spectral Theory*, 4(4):675–714, 2015.
- [7] Jeff Calder and Mahmood Etehad. Hamilton-jacobi equations on graphs with applications to semi-supervised learning and data depth. *Journal of Machine Learning Research*, 23(318):1–62, 2022.
- [8] Jeff Calder, Nicolás García Trillos, and Marta Lewicka. Lipschitz regularity of graph laplacians on random data clouds. *SIAM Journal on Mathematical Analysis*, 54(1):1169–1222, 2022.
- [9] Jeff Calder and Nicolás García Trillos. Improved spectral convergence rates for graph laplacians on ε -graphs and k-nn graphs. *Applied and Computational Harmonic Analysis*, 60:123–175, 2022.
- [10] Yueqi Cao, Didong Li, Huafei Sun, Amir H Assadi, and Shiqiang Zhang. Efficient weingarten map and curvature estimation on manifolds. *Machine Learning*, 110(6):1319–1344, 2021.
- [11] Thierry Champion, Luigi De Pascale, and Petri Juutinen. The ∞ -wasserstein distance: Local solutions and existence of optimal transport maps. *SIAM Journal on Mathematical Analysis*, 40(1):1–20, 2008.
- [12] Erik Davis and Sunder Sethuraman. Approximating geodesics via random points. *The Annals of Applied Probability*, 29(3):1446 – 1486.
- [13] Josep Diaz, Dieter Mitsche, Guillem Perarnau, and Xavier Pérez-Giménez. On the relation between graph distance and euclidean distance in random geometric graphs. *Advances in Applied Probability*, 48(3):848–864, 2016.

- [14] Manfredo Perdigao Do Carmo and J Flaherty Francis. *Riemannian geometry*, volume 6. Springer, 1992.
- [15] David B. Dunson, Hau-Tieng Wu, and Nan Wu. Spectral convergence of graph laplacian and heat kernel reconstruction in l^∞ from random samples. *Applied and Computational Harmonic Analysis*, 55:282–336, 2021.
- [16] Matthias Erbar and Jan Maas. Ricci Curvature of Finite Markov Chains via Convexity of the Entropy. *Archive for Rational Mechanics and Analysis*, 206(3), December 2012.
- [17] Hamza Farooq, Yongxin Chen, Tryphon T. Georgiou, Allen R. Tannenbaum, and Christophe Lenglet. Network curvature as a hallmark of brain structural connectivity. *Nature Communications*, 10, 2017.
- [18] Max Fathi and Jan Maas. Entropic Ricci curvature bounds for discrete interacting systems. *The Annals of Applied Probability*, 26(3), June 2016.
- [19] Lukas Fesser, Sergio Serrano de Haro Iváñez, Karel Devriendt, Melanie Weber, and Renaud Lambiotte. Augmentations of forman’s Ricci curvature and their applications in community detection. *arXiv:2306.06474*, 2023.
- [20] Forman, Robin. Bochner’s Method for Cell Complexes and Combinatorial Ricci Curvature. *Discrete & Computational Geometry*, 29(3):323–374, 2003.
- [21] Nicolás García Trillos. Gromov–hausdorff limit of wasserstein spaces on point clouds. *Calculus of Variations and Partial Differential Equations*, 59(2):1–43, 2020.
- [22] Nicolas García Trillos, Moritz Gerlach, Matthias Hein, and Dejan Slepčev. Error estimates for spectral convergence of the graph Laplacian on random geometric graphs toward the Laplace–Beltrami operator. *Foundations of Computational Mathematics*, pages 1–61, 2019.
- [23] Nicolás García Trillos and Dejan Slepčev. On the rate of convergence of empirical measures in infinity-transportation distance. *Canadian Journal of Mathematics*, 67(6):1358–1383, 2015.
- [24] Matthias Hein, Jean-Yves Audibert, and Ulrike von Luxburg. From Graphs to Manifolds – Weak and Strong Pointwise Consistency of Graph Laplacians. In Peter Auer and Ron Meir, editors, *Learning Theory*, Lecture Notes in Computer Science, pages 470–485, Berlin, Heidelberg, 2005. Springer.
- [25] C. Douglas Howard and Charles M. Newman. Geodesics and spanning trees for Euclidean first-passage percolation. *Annals of Probability*, pages 577–623, 2001.
- [26] Sung Jin Hwang, Steven B. Damelin, and Alfred O. Hero. Shortest path through random points. *The Annals of Applied Probability*, 26(5):2791–2823, 2016.

- [27] Jürgen Jost and Shiping Liu. Ollivier’s Ricci curvature, local clustering and curvature-dimension inequalities on graphs. *Discrete & Computational Geometry*, 51(2):300–322, 2014.
- [28] Kwang In Kim, James Tompkin, and Christian Theobalt. Curvature-Aware Regularization on Riemannian Submanifolds. In *2013 IEEE International Conference on Computer Vision*, pages 881–888. IEEE, December 2013.
- [29] Yong Lin, Linyuan Lu, and Shing-Tung Yau. Ricci curvature of graphs. *Tohoku Mathematical Journal*, 63(4):605 – 627, 2011.
- [30] Anna Little, Daniel McKenzie, and James M Murphy. Balancing geometry and density: Path distances on high-dimensional data. *SIAM Journal on Mathematics of Data Science*, 4(1):72–99, 2022.
- [31] Daniel Meyer and Eric Toubiana. Approximate Riemannian manifolds by polyhedra, April 2022. arXiv:2204.09536 [math].
- [32] Mervin E. Muller. A note on a method for generating points uniformly on n-dimensional spheres. *Commun. ACM*, 2(4):19–20, apr 1959.
- [33] Sumner B. Myers. Riemannian manifolds with positive mean curvature. *Duke Mathematical Journal*, 8(2):401 – 404, 1941.
- [34] Boaz Nadler, Stephane Lafon, Ioannis G. Kevrekidis, and Ronald R. Coifman. Diffusion maps, spectral clustering and eigenfunctions of Fokker-Planck operators. In *NIPS*, pages 955–962, 2006.
- [35] Chien-Chun Ni, Yu-Yao Lin, Feng Luo, and Jie Gao. Community detection on networks with ricci flow. *Scientific reports*, 9(1):1–12, 2019.
- [36] Yann Ollivier. Ricci curvature of markov chains on metric spaces. *Journal of Functional Analysis*, 256(3):810–864, 2009.
- [37] Yann Ollivier. A survey of Ricci curvature for metric spaces and Markov chains. In *Probabilistic Approach to Geometry*, pages 343–381. Mathematical Society of Japan, 2010.
- [38] Tim Roith and Leon Bungert. Continuum limit of lipschitz learning on graphs. *Foundations of Computational Mathematics*, 23(2):393–431, January 2022.
- [39] Sam T. Roweis and Lawrence K. Saul. Nonlinear dimensionality reduction by locally linear embedding. *Science*, 290(5500):2323–2326, 2000.
- [40] Romeil S. Sandhu, Typhon T. Georgiou, and Allen R. Tannenbaum. Ricci curvature: An economic indicator for market fragility and systemic risk. *Science advances*, 2(5):e1501495, 2016.

- [41] Amit Singer. From graph to manifold laplacian: The convergence rate. *Applied and Computational Harmonic Analysis*, 21(1):128–134, 2006. Special Issue: Diffusion Maps and Wavelets.
- [42] Joshua B. Tenenbaum, Vin de Silva, and John C. Langford. A Global Geometric Framework for Nonlinear Dimensionality Reduction. *Science*, 290:2319–2323, 2000.
- [43] Yu Tian, Zachary Lubbets, and Melanie Weber. Mixed-membership community detection via line graph curvature. In *Symmetry and Geometry in Neural Representations*, pages 219–233. PMLR, 2023.
- [44] Konstantin Usevich and Ivan Markovsky. Optimization on a grassmann manifold with application to system identification. *Automatica*, 50(6):1656–1662, 2014.
- [45] Pim van der Hoorn, William J Cunningham, Gabor Lippner, Carlo Trugenberger, and Dmitri Krioukov. Ollivier-Ricci curvature convergence in random geometric graphs. *Physical Review Research*, 3(1):013211, 2021.
- [46] Cédric Villani. *Topics in optimal transportation*, volume 58 of *Graduate Studies in Mathematics*. American Mathematical Society, Providence, RI, 2003.
- [47] Ulrike Von Luxburg. A tutorial on spectral clustering. *Statistics and Computing*, 17(4):395–416, 2007.
- [48] Melanie Weber, Jürgen Jost, and Emil Saucan. Forman-ricci flow for change detection in large dynamics data sets. *Axioms*, 5(4):doi-10, 2016.
- [49] Melanie Weber, Emil Saucan, and Jürgen Jost. Characterizing complex networks with forman-ricci curvature and associated geometric flows. *Journal of Complex Networks*, 5(4):527–550, 2017.
- [50] Melanie Weber, Emil Saucan, and Jürgen Jost. Coarse geometry of evolving networks. *Journal of Complex Networks*, 6(5):706–732, 2018.
- [51] Caroline L. Wormell and Sebastian Reich. Spectral convergence of diffusion maps: Improved error bounds and an alternative normalization. *SIAM Journal on Numerical Analysis*, 59(3):1687–1734, 2021.
- [52] Ze Ye, Kin Sum Liu, Tengfei Ma, Jie Gao, and Chao Chen. Curvature graph network. In *International Conference on Learning Representations*, 2020.